Title
STRUCTURE AND MECHANICAL PROPERTIES OF Fe-Cr-Co-C STEELS

Author
Raghavan, Mathur R.V.

Publication Date
1969-12-01

UCRL-19132

c.2

STRUCTURE AND MECHANICAL PROPERTIES OF Fe-Cr-Co-C STEELS

Mathur R. V. Raghavan
(M.S. Thesis)

December 1969

AEC Contract No. W-7405-eng-48

LAWRENCE RADIATION LABORATORY
UNIVERSITY of CALIFORNIA BERKELEY

UCRL-19132

DISCLAIMER

Contents

STRUCTURE AND MECHANICAL PROPERTIES OF Fe-Cr-Co-C STEELS

Mathur R. V. Raghavan

Inorganic Materials Research Division, Lawrence Radiation Laboratory
Department of Mechanical Engineering, College of Engineering
University of California, Berkeley, California

ABSTRACT

The structure and mechanical properties of tempered martensite and bainite in Fe-Cr-C steels with and without cobalt were investigated. The extent of twinning in the martensite of the steel without cobalt, having a higher M_s temperature, showed no significant difference from the one without cobalt which had a lower M_s temperature. Thus, M_s temperature of a steel is not the sole parameter controlling twinning. Autotempering was observed in the cobalt steel. All the steel showed an arrest in the yield strength and notch toughness when tempered in the 600-800°F range. Rapid softening occurred on tempering at 1000°F in all the steels. Cobalt did not exhibit any particular effect on tempering except that the cobalt steel had superior toughness only on tempering at 1000°F.

The isothermal transformations did not yield any superior product since the M_s temperatures of the steels were high, and the transformation yielded either a mixture of lower bainite and upper bainite or a mixture of tempered martensite and lower bainite depending upon the temperature of transformation. The transformation at 660°F gave optimum mechanical properties. The mechanical properties of the tempered martensite proved to be better than that of the isothermal transformation products. Continuous cooling of the steels did not result in any significant increase in the properties since the structure consisted of a mixture of bainite and martensite.

I. INTRODUCTION

In recent years considerable interest has been directed towards the production of high-strength steels with appreciable toughness. Many processes have been successfully developed recently[1,2,3] but all of them involve mechanical treatment besides heat treatment. It would be very attractive to develop high strength and high toughness by heat treatment alone. To start with, high strength could easily be obtained by increasing the carbon content of the steel, but this would seriously impair the toughness. The sharp decrease in toughness with increasing the carbon content of the steel should be accompanied by a marked change in the microstructure of the steel. The low carbon (less than .25%) martensite consists mainly of laths[4,5,6] with a high dislocation density. The striking change in the high carbon (more than 0.3%) martensite is that the structure consists mainly of plates rather than laths and many of the plates are internally twinned. These transformation twins in martensite are due to the lack of slip at the temperatures of formation of the martensite. The formation of twins in the high carbon steels are associated with a decrease in the M_s temperature of the steels. Based on experimental evidence, many workers[7,8,9] suggested that the M_s temperature of the steel could be the deciding factor for twinning. If this is true, it should be possible to eliminate the formation of twins in the martensite by raising the M_s of the steel. It has been suggested[5,10] that the presence of twins could seriously affect the fracture toughness which, in turn, would imply that the M_s temperature is a key parameter in controlling the twinning and hence the fracture toughness. So, this brings to mind two questions:

1. Does the M_s temperature control the twinning?

2. Do the twins decrease the notch toughness?

A definite answer to these questions adds a new dimension to the alloy design. The aim of the present investigation was to find a suitable answer to the above questions and to correlate the mechanical properties with the structure of tempered martensite and bainite. Two steels with the same carbon (.35% C) and chromium (4% Cr) but one without cobalt and the other with 5.3% cobalt were chosen. Since cobalt is known to raise the M_s, the steel with cobalt had a higher M_s compared to the one without cobalt. A third steel representative of a low carbon steel was also chosen.

A brief study of the mechanical properties of the tempered martensite and bainite was done to evaluate their relative merits and demerits. It had been shown[11-15] conclusively that in a high carbon steel, the mechanical properties of the tempered martensite (which had twins in them) were inferior to that of the bainite structures that were twinfree.[16,17] However, contradictory observations have also been made.[19-21] In the low carbon steels, tempered martensite, having no twins, was superior to the bainite product.

II. EXPERIMENTAL PROCEDURE

A. Heat Treatment

The ingots were placed in cast iron tubes packed with cast iron chips to prevent decarburization and then homogenized at 2300°F for three days. Pieces were cut from the homogenized ingots, forged, and finally rolled to the required thickness.

The specimens were homogenized in an argon atmosphere at 1800°F for an hour and then quenched directly into water. They were immediately transferred to a liquid nitrogen dewar and stored there for about an hour to ensure complete transformation of the untransformed austenite. For tempering and isothermal transformations, low-temperature salt baths were used, operating in the range of 350°F to 1050°F. Tempering was done at four different temperatures for 4 hours followed by quenching in water. For isothermal transformations, the specimens were directly quenched into the salt bath operating at the required temperature and then held for the required period. The heat-treated specimens were sandblasted to remove any decarburized layer. For continuous cooling studies, the specimens were dropped out of the furnace after homogenization and then were allowed to cool in air.

B. Mechanical Testing

Figures 1a and b show the dimensions of the tensile specimens and substandard Charpy impact specimens used. Tensile tests were performed in an Instron machine with a cross-head speed of .0423"/sec (.1 cm/min). Impact testing was performed using a substandard Charpy impact machine using a 16-ft-lb hammer. The impact values listed in the tables thus correspond to the 16 ft-lb hammer.

C. Electron Microscopy

Specimens for the electron microscopy were about 30 to 40 mils thick and were heat-treated together with the tensile and impact specimens. The bulk specimens were then chemically thinned in H_2O_2 containing 2% HF at room temperature. The solution was cooled with water to avoid temperature rise which would result in explosion. The specimens were thinned chemically to about 4 mils thick and then electropolished. Disks of the size of the standard Siemens specimen holder were punched and then polished in a twin-jet polishing apparatus. Electropolishing was done using a chromic-acetic acid solution (75 gms CrO_3 + 400 ml acetic acid + 20 ml of distilled water). The voltage varied from 19-25 volts and the current varied from 12-16 milliamps. The polishing conditions, however, depended on the jet speed and the spacing between the jets. Normal polishing time was about three minutes depending on the thickness of the initial disk. The disks were then examined in a Siemens Elmiskop I microscope operating at 100 kV.

D. Electron Fractography

A two-stage plastic-carbon replica was employed for fracture studies. The fracture surfaces of the Charpy specimens were replicated with cellulose-acetate tape followed by shadowing with chromium chips at 45° angle to the surface, and finally carbon was normally evaporated on the surface. The tape was then dissolved in acetone and the carbon film was dried and examined at 80 kV and at a magnification of 6000x.

III. RESULTS

A. Mechanical Properties of Tempered Martensite

Table I lists the compositions of the steels investigated along with their heat numbers. Table II indicates the mechanical properties of the tempered steels. Figures 2, 3, and 4 show the variation of the mechanical properties on tempering for steels 12, 26 and 24 respectively. Figure 5 summarizes the response of all the steels to tempering. All the steels showed similar behavior on tempering. When tempered at 400°F, the tensile and the yield strengths decreased with an attendant increase in ductility and notch toughness. On tempering in the range of 600-800°F, the yield strength and notch toughness values remained constant for all the steels, followed by a rapid softening when tempered at 1000°F. Steel 26 showed better toughness (when compared to that of steels 12 and 24) when tempered at 1000°F. In general, the toughness values of the steels were poor until 800°F tempering after which all the steels showed a rapid increase in toughness and a corresponding decrease in strength.

It is of special interest to note that the yield strength of all the steels decreased considerably on tempering at 400°F and then remained fairly constant until 800°F, followed by a decrease when tempered at 1000°F. This suggests that in the 600-800°F tempering range, the normal softening tendency was counteracted by a strengthening mechanism resulting in no significant net change in the strengths. Again, on tempering at 1000°F the strength decreased because the softening mechanism became predominant. The notch toughness values also showed a slight increase on tempering at 400°F, then remained constant (or slightly decreased) on tempering until 800°F and then increased considerably on tempering at 1000°F. When the mechanical properties of steel 12 (no cobalt) and steel 24 (1.4% co) were

compared (fig. 5), it was found that steel 24 showed better properties. This improvement in the mechanical properties could be attributed to the cobalt addition in steel 24. However, this increase in the mechanical properties with the cobalt content of the steel was not linear since increasing the cobalt content from 1.4% (in steel 12) to 5.3% (in steel 26) did not show any improvement in the properties. The solid solution strengthening of cobalt could not be estimated since the carbon contents of all the steels were different and the solid solution strengthening of cobalt cannot be distinguished from that of carbon.

B. Mechanical Properties of Isothermal Transformation and Continuously Cooled Products

Isothermal transformations were carried out at five different temperatures, namely 840°, 750°, 660°, 570°, and 480°F for 24 hours. In some cases the transformations were carried out for 75 to 100 hours. Table III lists the mechanical properties of the isothermal products. In general, the mechanical properties of isothermally decomposed steels were inferior compared to the mechanical properties of tempered martensite. With increasing transformation temperature, the yield strength showed a decrease and the toughness values showed a maximum at the transformation temperature of 660°F. Isothermal transformation at other temperatures had inferior toughness. Fig. 6 shows the mechanical properties of the isothermal products at different isothermal temperatures. Fig.7 summarizes the properties of both tempered and isothermally transformed steels.

Continuous cooling studies showed that steel 12 had a higher strength and lower toughness where steel 26 exhibited lower strength and high toughness. Steel 24 had properties in between steels 12 and 26.

C. Structure of Martensites

Electron microscopy study shows that the martensites of steel 12 and 26 showed little difference in twinning. The former had no cobalt and had a lower M_s temperature compared to the latter (see table 1). Since both the steels 12 and 26 had approximately the same carbon contents (.35%) the martensite mainly consisted of twinned and untwinned plates. The extent of twinning was not the same in all the plates but varied widely from plate to plate. Fig. 8 shows the asquenched structures of steel 12. Fig. 8a shows extensive twinning and fig. 8b the dark field image where the twins reverse contrast. By increasing the carbon content of the steel, the volume fraction of such extensive twins was found to increase.[11,12] Fig. 8e is the bright-field micrograph of an adjacent region having relatively fine twins. Fig. 8f shows the bright field image of twins in a plate marked A. The adjacent plate is marked B. The dark field image of (200) spot shows the reversal of contrast of the twins, as well as of plate B. This proves that plates B and A are twin related. Besides the twins, some substructures were also observed, marked. B in fig. 8h; and the dark field micrograph of the $(1\bar{1}0)$ spot reverses contrast of the twins and substructures (fig. 8j). Thus, these substructures are also twin related with the matrix A. Fig. 9 shows the asquenched structure of steel 26 which has 5.3% Co. The structure was not very different from steel 12. Again the structure varied from extensively twinned plates (fig. 9a) to very fine twins (fig. 9b). In some areas even dislocated martensite was observed (fig. 9c). The only striking change in steel 26 was the auto-tempered precipitates. Fig. 9d shows the bright field picture of a plate and the carbides that are barely visible. Fig. 9e shows the dark field picture where the carbides reverse contrast. The carbides were fairly

spherodized and hence it was not possible to trace analyze the carbides. However, earlier reports[11,22] have shown that the precipitates are cementite, but autotempered ε-carbide precipitates have also been reported.[23] An important observation would be that the autotempered precipitates were not observed in any of the twinned plates, but were frequently observed in untwinned plates. The importance of this shall be discussed later. Selected area diffraction patterns of the dislocated martensite in the steels clearly indicate that laths are not twin related with respect to each other.

D. Structure of Tempered Martensite

On tempering at 400°F, cementite started precipitating in the matrix accompanied by precipitation along the twins. In some regions, wavy ε-carbide was also observed. Since the carbide diffraction spots were too weak, the carbides were identified by trace analysis. It has already been established that cementite forms on {110} planes of martensite and ε-carbide forms on {100} planes of martensite.[24,25] Most of the carbides were cementite, and precipitation of cementite in the matrix was of the typical Widmanstatten type. Figs. 11d-g show precipitation of cementite in two sets of planes. Regions marked A in fig. 11d and B in fig. 11e were ε-carbides lying along {100} trace. The ε-carbides were wavy in nature unlike sharp precipitates of cementite. Figs. 11f and g show the bright and dark field pictures of cementite. Though cementite precipitation at the twin boundaries was observed, no plate boundary precipitation was detected.

While the cementite precipitation in an untwinned plate was of the Widmanstatten type, the carbide morphology was considerably altered by the presence of twins. Twin boundary precipitation of cementite started from

400°F tempering. These twin proboundary precipitation, in effect, resulted in the formation of long carbides along the twins and across the plates. Observations showed that the cementite nucleated discontinuously along the twins and they subsequently grew to form continuous carbides, thus forming long barriers across a plate. The reason the twins act as suitable sites for the nucleation of carbides has been discussed by Tekin and Kelly.[24]

Plate boundary carbide precipitation was observed at 600°F tempering (fig. 12). At all tempering temperatures above 600°F carbide precipitation as well as general matrix precipitation occurred along twin boundaries, plate boundaries and austenitic grain boundaries. With increasing temperatures, the matrix precipitates started spheroidizing and also the precipitates along the imperfections were coarse. Figs. 13 a, b are the dark field pictures showing clear plate boundary carbide precipitation and matrix precipitation (fig. 13c) which had started to spherodize. Fig. 14a shows the bright-field picture of steel 12 tempered at 1000°F, showing spherodized carbides which reverse contrast in the dark field image (fig. 14b). Fig. 14b is the dark field picture of $(01\bar{1})$ spot but since both the matrix and carbides reverse contrast in the dark field image, a carbide spot is superimposed on the $(01\bar{1})$ matrix spot. Coarse carbide precipitation along the twins is indicated in fig. 14c by an arrow, and grain boundary carbide precipitation is shown in fig. 14d. Fig. 15 represents the structure of steel 26 tempered at 1000°F. Plate boundary is evident in fig. 15a (marked by arrow) whereas regions marked A in fig. 15b are the carbides on the twins. Fig. 15c is a dark field image of a carbide spot showing spherodized carbides reversing contrast.

Thus, even after tempering at 1000°F the twins were not removed since the temperature was not high enough for recrystallization. There was no significant difference in the structures of steels 12 and 26, indicating that cobalt did not affect the tempering characteristics of the steels.

E. Structure of Isothermal Transformations and Continuously Cooled Products

Electron microscopy studies of steel 26 revealed that transformation conducted at 750°F yielded a mixture of upper and lower bainite (fig. 16) and when transformed at 840°F, the structure consisted exclusively of upper bainite (fig. 17). At temperatures below M_s, the isothermal transformation yielded a mixture of tempered martensite and lower bainite (not shown here).

The lower bainite consisted of acicular ferrite with the carbides at an angle of 55-65° to the long direction of ferrite laths as already reported.[26,27] The upper bainitic structures in these steels are similar to the ones already observed.[27] The structure consisted of laths of bainite with carbide precipitation at the lath boundaries. The carbides in lower bainite were found to precipitate on the $\{112\}_\alpha$ planes but frequently $\{110\}_\alpha$ habit were also observed (fig. 16d). The transition from lower to upper bainite occurred at the temperature range of 750-850°F.

It has already been pointed out[28] that the substitutional atoms in steel do not contribute to the carbides that form in bainite, and hence the carbides that form are cementite. Fig. 16e shows a diffraction pattern of the bainitic carbides and fig. 16f shows the crystallographic relation between the cementite and ferrite lattices, which corresponds

to the Bagaryatskii orientation relationship as was already pointed out,[27,29] and is as follows:

(100) cementite // ($0\bar{1}1$) ferrite (001) cementite // (211) ferrite
(010) cementite // ($1\bar{1}\bar{1}$) ferrite

Continuously cooled structures consisted mainly of bainite (figs. 16-19). In steel 12, a mixed structure of upper bainite, lower bainite and martensite was observed. Fig. 18a shows the bright field image of the upper bainite formed during continuous cooling anf fig. 18b is the dark field micrograph where the carbides at the plate boundaries reverse contrast. Lower bainitic structures were also frequently observed as in fig. 18c. When dislocated martensite was present it was difficult to distinguish it from the bainitic laths which did not show pronounced carbide precipitation. However, frequent martensite plates were observed having tempered carbides in them and were similar to tempered martensite. Fig. 18d shows one such bright field micrograph. Presence of ε-carbide was observed by trace analysis and are indicated by arrows. When the martensite formed was twinned, it could be very easily distinguished from the bainite. Fig. 18e shows a similar situation and the twins in martensite are marked by arrows. Thus, though more dislocated martensite could have been present, it could not be distinguished from bainitic laths. The width of the bainite laths were very fine compared to the ones formed isothermally and the carbides were also finer in the continuously cooled steel (compare figs. 17 and 18a).

Continuously cooled structure of steel 26 also consisted of a mixture of lower and upper bainite with more of lower bainite. No martensite was observed. Again the carbides formed were finer than the carbides formed isothermally (combine fig. 16a and 19a). Fig. 19a shows

lower bainite structure where again the carbides had habits varying between (110) and (121).

F. Fractography Studies

Fig. 20a is the fractograph of steel 12 asquenched and shows cleavage rupture whereas fig. 20b is the same steel tempered at 1000°F and hence shows a typical dimpled rupture. Fig. 21 is the fracture surface of steel 12 tempered at 600°F where the arrest in the yield strength had occurred. This again shows a dimpled rupture and not cleavage. Since the steel tempered at 600°F did not show any predominant intergranular failure, it indicated that the failure was not due to any grain boundary carbide precipitation.

IV. DISCUSSION

A. Morphology of Martensites

Martensites of steels 12 and 26 showed little difference in twinning denoting that M_s is not the only parameter affecting twinning. The belief that M_s controlled twinning failed to answer why a Fe-Ni martensite twins at about 28% Ni content when the M_s is below room temperature whereas a Fe-C martensite twins at as low as 0.3% C when the M_s is about 700°F. Thus carbon has a direct effect in twinning other than decreasing M_s. Other workers[33] debated that ΔG, the free energy change of the $\gamma \rightarrow \alpha$ transformation would be the deciding factor and twinning would occur when the composition of the steel was such that the driving force at M_s attained a critical value of 300 to 370 cals/mole. Again, Bell and Owen[34] suggested that in Fe-C and Fe-N systems the transition from dislocated to twinned martensite occurs when a critical driving force of 315 cals/mole was reached. But the authors[33] could not confirm this theory in Fe-Cr system when they failed to observe any twinning at 5% Cr where the ΔG was 300 to 350 cals/mole. It would thus appear also that ΔG is not a key parameter in deciding twinning.

Electron microscopy observations showed that in steel 26 autotempered carbides formed only in the untwinned plates. Autotempering occurs below M_s (provided the M_s temperature is high enough to effect carbide precipitation) in the plates that form first. This indicates that at temperatures at which autotempering occurs, the CRSS is favorable for slip resulting in twin free plates. However, at lower temperatures when autotempering does not occur, CRSS is favorable for twinning and hence

the martensite twins. Thus, the temperature at which the plates form affects the CRSS which in turn decides whether the plates will twin or slip. However, there is some ambiguity when the extent of twinning is correlated with the size of the martensite plates. According to the earlier arguments, the plates that form just below M_s would be relatively less twinned than the plates formed later. One would expect the plates that form first to be the largest. Similarly, the plates formed at lower temperatures would be more twinned. General observation shows that this is not always true. Notwithstanding, it is difficult to assert that the last formed plates are the smallest since the possibility of formation of small plates at high temperatures cannot be excluded. Besides, the size of the plates formed may not continuously decrease from M_s to M_f. Hence, in spite of the fact that the correlation of plate size with twinning is not very promising, other evidences (like autotempering) indicate that the temperature of formation of martensite may decide the relative extent of twinning.

In interpreting the autotempering effects in the steels, one should be very careful about the variables. For instance, autotempering depends not only on the M_s temperature, but also on the thickness of the specimens quenched. Normally the thin foils prepared from bulk samples represent the interior of the bulk samples and not the surface. Thus, if the specimen quenched is thicker, the interior cools at a slower rate resulting in more autotempering in the thin foil studies. The correlation of autotempering with M_s, hence should not be done with specimens of varying thicknesses. Experiments conducted by Page[22] on a steel similar to steel 12 (but with lower carbon) showed extensive autotempering. The bulk specimens heat treated were about 100 mils thick. Though the M_s of these steels

were higher than the present steels under investigation, the thickness of the heat-treated specimens would have been equally important in deciding the extent of autotempering.

In the low carbon martensite, the laths are frequently separated by low angle boundaries. In the high carbon martensite the strain energy of the transformation $\gamma \rightarrow \alpha$ cannot be accommodated by low angle boundaries between the plates and hence the system reduces its strain energy by forming twin related plates. However, it seems that the plates are not only twin related with respect to each other but that the other structures (fig. 8h) are also twin related with the plates in which they form.

B. Morphology of Isothermal Transformation Products

The structure of steel 26 isothermally transformed at 840°F consisted mainly of upper bainite. According to Pickering,[29] in a .35% C steel this temperature should be of the order of 980°F. This discrepancy could be explained due to the alloying elements in the steel[26] since Pickering's investigations were on plain carbon steels.

Since no twinning was observed in the lower bainite, the precipitation of carbides on the {112} planes cannot be explained. In some cases precipitation along {110} was also observed which corresponds to the cementite habit in tempered martensite. The argument[27] that twins can be removed by carbide precipitation is not likely since even tempering at 1000°F did not remove the twinning.

In spite of the fact that the steels tempered at 1000°F show carbide precipitation at the twins and plate boundaries, they do not show any arrest in the mechanical properties. This indicates that the carbide precipitation at the twins and plate boundaries is not responsible for

the observed arrest that occurred in the tempering range of 600-800°F. However, some toughness would definitely be lost due to these precipitations. For instance, it appears that the carbide precipitation along the twins would promote transgranular failure compared to the situation when the twins are carbide free, but this effect does not seem to be predominant. Moreover, since all the steels exhibit the arrest in the mechanical properties, it is obvious that cobalt has no special role in this arrest.

C. Structure and Mechanical Properties of Tempered Martensite

Electron microscopy evidence shows that on tempering at 400°F there was no plate boundary precipitation but that precipitation at twin boundaries had started (fig. 11a). Tempering at 600°F, however, showed that carbides started precipitating at the plate boundaries (fig. 12). The twin boundary and plate boundary carbide precipitation was observed at all tempering temperatures above 400°F (figs. 12, 13a,b, 14c, 15a,b). Also, fractographic studies made clear that the fracture path was not intergranular but was primarily transgranular dimpled rupture (fig. 21).

Tempering in the 600-800°F range arrested the normal variations in yield strength and notch toughness. It has already been mentioned that a strengthening mechanism could operate when tempered in this range which counteracted the normal softening tendency and held the yield strength fairly constant. This strengthening mechanism also caused an arrest in the notch toughness values.

Referring to the microstructures of the tempered steels, the steels tempered at 400°F show the presence of ε-carbides. Since the nucleation of cementite does not occur insitu, it has been suggested that cementite nucleates separately and these fresh carbides form on dislocations, jogs,

etc., restirct their mobility and hence affect the toughness. Had this been true, the arrest should have occurred at 400° itself since the majority of the carbides ar 400°F were cementite. Thus, it may be concluded that the fresh nucleation of cementite is not the factor causing the arrest.

Reports on secondary hardening by Bain and Paxton[35] show that though a 4% Cr, 0.35 C steel does not exhibit any pronounced secondary hardening, there is a definite change in the hardness versus tempering temperature curve. In other words the tempering of this steel in the range of 600-800°F is accompanied by precipitation of chromium carbides which causes secondary hardening (though not pronounced). It has been conclusively shown that secondary hardening is a function of both carbon and chromium content. If the carbon content of steel is high (about .4%), then significant secondary hardening occurs at as low as 3% chromium content, whereas with .35% C only 4% Cr produces slight hardening. The reason Page[22] failed to observe any secondary hardening in his steel (Fe-4% Cr-0.18% C) was because of the low carbon content of his steel. Again the tempering at 600-800°F only arrests the yield strength and notch toughness values but neither causes an increase in yield strength nor a decrease in toughness. This is because the secondary hardening is not pronounced; but with higher Cr or C contents the effect would be more prominent showing a clear increase in strength and decrease in toughness. Further support to the above argument can be claimed from the fact that the hardening reported in 4% Cr .35%C steels[35] occurs in 600-800°F tempering range, which is the same as observed in the present investigation. Thus, the formation of chromium carbides seem to be the proper explanation to the observation. Unfortunately, electron microscopy evidence cannot be produced to prove

that the carbides are chromium carbides due to the lack of a carbide diffraction pattern. At these high tempering temperatures, the carbides spherodize considerably and it is almost impossible to trace analyze these carbides. However, x-ray micro-analysis on the extracted carbides will be conducted to identify the carbides. Since cobalt is not a carbide forming element, it doesn't affect the formation of chromium carbides. Thus, the very fact that the chromium content in all the steels is the same, all of them exhibit the hardening phenomenon irrespective of their cobalt contents.

The rapid softening that occurs at 1000°F needs considerable attention. Normally one would expect to have complete recrystallization of the structure for such a softening. Fig. 15b shows the bright field image of carbides, and regions marked A show the carbides that had formed on twins. Fig. 15c shows spherodized carbides reversing contrast. Other regions (not shown here) also exhibited twinning which clearly indicate that twins had not been removed even at that high tempering temperature. Thus, the softening could only be due to the fact that the carbides had completely spherodized and the matrix was very soft due to complete depletion of carbon from it. This only explains why all the three steels rapidly soften on tempering at 1000°F but it does not explain why the cobalt steel should show a more rapid increase in toughness.

D. Mechanical Properties of Isothermal and Continuously Cooled Products

The M_s temperatures of the steels investigated are in the range of 660-750°F (Table I). Isothermal transformation carried out above this temperature yields bainite and below this temperature, a mixture of bainite and martensite, tempered at the temperature of holding. In view

of the high M_s temperature of these steels, isothermal transformation yields inferior mechanical properties as indicated in fig. 7. This does not mean that in high carbon steels tempered martensite has better mechanical properties than that of bainite because one never gets 100% lower bainite in these steels. The M_s is so high that isothermal transformation at M_s yields a mixture of upper and lower bainites with more of lower bainite. An increase in the transformation temperature would obviously increase the proportion of upper bainite which is not desirable. A decrease in the transformation temperature would cause the formation of (twinned) martensite and yield a mixture as mentioned already. From fig. 6 it is clear that on increasing the transformation temperature from 570-660°F the notch toughness increased and then decreased as the temperature was increased from 660-750°F. The increase in notch toughness is due to the increasing proportions of lower bainite and a corresponding decrease in the amount of tempered martensite. But this increase is compensated by the fact that increasing transformation temperature decreases the toughness of the lower bainite formed.[11,12] However, it seems that the increase in toughness overweighs the corresponding decrease and hence one observes a finite, though small, increase in toughness. On increasing the transformation temperature, upper bainite replaces lower bainite over a range of temerature and the toughness decreases again. The optimum transformation temperature seems to be around 660°F which strikes a good compromise among these phases. Thus, while the isothermal transformation at higher transformation temperature is impaired by upper bainite, the steel transformed at lower (below M_s) temperature is embrittled by the presence of tempered twinned martensite. Since a 100% lower bainite could not be formed in these steels, a direct

evidence of superiority of bainite cannot be claimed. Notwithstanding, this could be seen indirectly since the toughness increased with the decreasing amount of tempered martensite.

The variation in toughness described above could not possibly be due to virgin martensite that could have formed from the untransformed austenite on cooling to room temperature after transformation because prolonged holding at that temperature did not result in any significant change in properties (Table III). However, this point will be checked to confirm the argument.

The vast difference in the properties of continuously cooled steel 26 and steel 12 could possibly be due to the untransformed austenite that ultimately transformed to martensite. Since the TTT curve of steel 26 was to the left of the curves of steel 12, possibly the bainite transformation did not go to completion in steel 12 and hence the steel was embrittled due to martensite. Steel 26 consisted mainly of lower bainite and some upper bainite and practically no martensite could be detected. The steel hence showed better toughness. Moreover, the finer bainitic laths could also have contributed to the toughness.

E. Effect of M_s on Twinning

A direct correlation between M_s and twinning is hard to conceive for all the steels. The alloying elements in a steel not only alter the M_s temperature of the steel, but also affect many other factors. Thus, by fixing M_s as a parameter, one obviously overlooks the other changes that have occurred besides the change in M_s. The endeavor to make the CRSS favorable for slip by increasing the temperature at which martensite starts forming (by cobalt additions) is not likely to be successful. This is because the CRSS is not only affected by temperature, but is also

affected by the alloying elements. Any solute element would invariably increase the stress required to slip. This increase may not be very appreciable with substitutional elements like Cr, Ni, Mn, etc., but the interstitial elements such as carbon would cause a tremendous increase. Although the increase in the M_s temperature of the steel with cobalt decreases the CRSS for slip of martensite, this decrease in CRSS for slip may be compensated for by increase in CRSS due to solid solution effect of cobalt. Thus, the martensites of steels with and without cobalt show little difference in twinning. The effect of solute elements on the twinning stress should also be considered. Not much work has been done on this topic. Notwithstanding, the effect of solute elements on CRSS for slip is expected to be more pronounced than their effect on CRSS for twinning. Carbon has a tremendous effect on CRSS for slip compared to Ni and this could be the reason why, at the same M_s temperature, a Fe-C martensite shows more twinning than a Fe-Ni martensite. Thus, the M_s temperature of a steel is not an absolute measure of the twinning in the martensite.

F. Effect of Twinning on Toughness

Earlier works[11,12] indicate that twinned structures do not have superior notch toughness as compared to the twin free bainite structure. Thus, in a high carbon steel a twin free bainite structure is preferred to twinned tempered martensite and the reverse is true in a low carbon steel. Moreover, the mode of deformation of martensite is important. In high carbon steels (above .04% C) the mode of deformation of martensite has been shown[30,31] to be twinning. Thus, besides the fact that transformation twins result in poor notch toughness, they also intersect with the deformation twins and give rise to microcracks,[32] which are

detrimental to the mechanical properties of the steel. Thus, a high carbon steel is disadvantageous in these two ways. When a high carbon steel is tempered, the carbon content of the matrix is reduced so that the martensite deforms by twinning. Thus, in tempered steels the deformation made is less likely to be twinning. However, the question whether the transformation twins affect the mode of deformation still remains to be answered. The inferior toughness of the twinned structures (compared to the toughness of twin-free bainite) cannot be attributed to the deformation mode, but the transformation twins definitely affect the toughness. The transformation twins in the asquenched martensite alter the morphology of the subsequent carbide precipitation on tempering. Thus, the nucleation of cracks due to pile-up of dislocations at the carbides would seem to be a plausible mechanism of decreasing toughness. In the steels, one cannot evaluate the effect of twins on the toughness because the carbide morphology comes into play on tempering. Even the toughness of the asquenched martensites with and without twins do not give any indication of the effect of twins because even if the high carbon martensite is less tough (as is always the case), it does not indicate that the twinning in the high carbon martensite causes the inferior toughness. This is because the solid solution effect of carbon is very pronounced and thus it is impossible to distinguish its effect on toughness from the effect of twins on toughness. The toughness values of Fe-Ni alloys with and without twins (high and low Ni alloys respectively) would indicate the effect of twins on toughness since the solid solution effect of Ni is not as pronounced as carbon. Thus, in order to investigate the effect of transformation twins on toughness, all other factors (like carbide, morphology, etc.) should be eliminated.

V. CONCLUSIONS

1. An increase in M_s temperature does not decrease twinning and hence M_s is not the sole factor determining twinning. Thus, two steels having the same M_s temperature, but different composition need not exhibit the same extent of twinning.

2. Although M_s is no indication of twinning when comparing two different steels, in the same steel the temperature at which martensite forms, which varied from M_s to M_f, determines the extent of twinning in the plates. Plates formed initially were less twinned compared to the ones formed later at lower temperatures.

3. Twinned structures have inferior mechanical properties compared to untwinned structures.

4. It does not seem practicable to produce a high carbon twin-free martensite in the normal structual steels.

5. A finite (though small) increase in toughness in the high cobalt steels over the straight chromium steel can be attributed to the autotempering observed in these steels.

6. All the steels show similar changes in the mechanical properties on tempering. The high cobalt steel has higher toughness than the others on tempering at 1000°F.

7. Since all the steels exhibit an arrest in the mechanical properties when tempered in the 600-800°F region, cobalt has no effect in the arrest.

8. The observed arrest in the mechanical properties is not due to plate boundary or twin boundary precipitation of carbides.

9. The arrest in the mechanical properties of all the steels when

tempered in the 600-800°F region could be due to the formation of chromium carbides in this temperature range. All the steels exhibit this arrest since all of them have 4% Cr.

10. In steels having high M_s temperatures, isothermal transformations do not yield superior products due to the interference of upper bainite. In such steels, tempered martensite has better mechanical properties (in spite of the twinned structure).

11. An isothermal transformation temperature of 660°F shows optimum mechanical properties.

12. Continuous cooling of cobalt steels yields a tougher and a lower yield strength steel compared to the straight chromium steel which is brittle due to martensite.

13. Bainite laths and carbides formed during continuous cooling are finer than the ones formed by isothermal transformations.

14. Addition of cobalt in excess of 1.4% does not result in any improvement in the mechanical properties.

Acknowledgements

The author is deeply grateful to Professors Gareth Thomas, Victor Zackay and Earl Parker for their personal guidance, encouragement and support throughout the course of this work.

Special thanks are due to Mr. W. W. Gerberich and Mr. Santosh Das for valuable discussions and help during the course of this work. Thanks are due to Shirley Ashley and Carol ZumBrunnen for their help in typing, and Phila Witherlla for her help in photography.

This work was done under the auspices of the U.S. Atomic Energy Commission through the Inorganic Materials Research Division of the Lawrence Radiation Laboratory.

REFERENCES

1. V. F. Zackay, E. R. Parker, D. Fahr, and R. Busch, Trans. ASM 60, no. 2, 252 (1967).
2. E. W. Page, P. Mangonon, G. Thomas, and V. F. Zackay, Trans. ASM 62, 45 (1969).
3. G. Thomas, D. Schmatz, and W. Gerberich, High Strength Materials, ed. V. F. Zackay, J. Wiley and Sons, New York 199 (1965).
4. G. R. Speich and H. Warlimont, J. Iron and Steel Inst., 206, 385 (1968).
5. P. M. Kelly and J. Nutting, J. Iron and Steel Inst. 197, 199 (1961).
6. P. M. Kelly and J. Nutting, Proc. Roy. Soc. (A) 259, 45 (1960).
7. O. Johari and G. Thomas, Acta Met. 13, 1211 (1965).
8. K. W. Andrews, J.I.S.I., 721 (1965).
9. R. L. Patterson and C. M. Wayman, Acta Met. 12, 1306 (1964).
10. A. S. Tetelman, Discussion: High Strength Materials, ed. V. F. Zackay, John Wiley and Sons, New York, 324 (1965).
11. S. K. Das, M.S. thesis, University of California, 1968.
12. D. H. Huang, M. S. thesis, University of California, 1969.
13. E. S. Davenport, E-L. Roff, and E. C. Bain, Trans. ASM 22, 289 (1934).
14. B. J. Waterhouse, Discussion, Physical Properties of Martensite and Bainite, Special Report 93, The Iron and Steel Institute (London) 147 (1965).
15. R. F. Hehemann, V. J. Lahan, and A. R. Trocano, Trans. ASM, 49, 409 (1957).
16. G. R. Srinivasan and C. M. Wayman, Acta Met. 16, 609 (1968).
17. K. Shimizu, J. Ko and Z. Ni Shiyama, Trans. Japan Inst. of Metals 5, 225 (1964).

18. J. M. Oblak and R. F. Hehemann, Symposium: Transformation and Hardenability in Steels, Climax Molybedenum Co., 15 (1967).

19. J. H. Hollman, L. D. Jaffe, D. E. McCarthy, and M. R. Norton, Trans. ASM, 38 807 (1947).

20. S. A. Herres and C. H. Lorig, Trans. ASM 40, 775 (1948).

21. G. Sachs, L. J. Ebert and W. F. Brown, Trans AIME 176, 424 (1948).

22. E. W. Page, M. S. thesis, University of California, 1968.

23. B. R. Banerjee, J. Iron and Steel Inst. 203, 166 (1965).

24. E. Tekin and P. M. Kelly, Precipitation from Iron-Base Alloys, eds. G. R. Speich and J. B. Clark, Gordon and Breach Science Publishers, New York (1965).

25. M. G. H. Wells, Acta Met., 12 (1964) 389.

26. Second Progress Report by Subcommittee XI of Committee E-4, Electron Microstructure of Bainite in Steel, ASTM Proc. 52, 543 (1952).

27. D. N. Shackleton and P. M. Kelly, The Iron and Steel Inst. (London) Report 93, 126 (1965).

28. R. E. Reed Hill, Physical Metallurgy Principles, Van Nostrand Co. 1964.

29. F. B. Pickering, Symposium: Transformation and Hardenability in Steels, Climax Molybdenum Co. (1967).

30. G. Krauss and W. Pitsch, Acta Met. 12, 278 (1964).

31. R. H. Richman, Trans. AIME 227, 159 (1963).

32. D. Hull, Acta Met. 8, 11 (1960).

33. J. S. Pascover and S. V. Radcliffe, Trans. AIME 242, 673 (1968).

34. T. Bell and W. S. Owen, Trans. TMS-AIME, 239, 1940 (1967).

35. E. C. Bain and H. W. Paxton, "Alloying Elements in Steel," ASM, 1966.

36. J. Hall, M. S. thesis, University of California, 1968.

Table I

	Heat No.	Composition				M_s* temp.
		% Cr	% C	% Co	% Fe	°F
1	12	4	0.343	0	bal	660
2	26	4	0.351	5.3	bal	735
3	24	4	0.281	1.4	bal	725

Table II

Mechanical Properties of Asquenched, Tempered, and Aircooled Structure

Heat No.	Heat Treatment Tempering Temperature (°F)	U.T.S. ksi	Y.S. ksi	% El	Charpy Impact value * (ft-lbs)
	Asquenched	265	219	4.4	0.30
	400	219	179	4.6	0.70
12	600	212	175	4.5	0.70
	800	197	172	4.0	2.00
	1000	168	146	7.3	7.40
	Normalized	243	185	5.0	0.90
	Asquenched	258	209	5.0	0.60
	400	217	177	4.8	1.00
26	600	211	179	5.2	0.80
	800	189	168	6.6	1.70
	1000	162	142	7.7	10.50
	Normalized	172	150	6.0	3.60
	Asquenched	268	216	--	0.30
	400	225	180	5.0	1.90
24	600	216	181	4.60	1.00
	800	189	163	6.40	3.00
	1000	161	142	7.20	9.60
	Normalized	200	166	4.30	2.50

*Substandard Charpy impact specimens using a 16 ft-lb hammer.

Table III

Mechanical Properties of Isothermal Transformations

Steel	Temperature °F	Time (Hvs)	Tensile strength ksi	Yield strength	% Elongation	Charpy Impact value* (ft-lbs)
	480	75	232	190	5.5	0.8
		100	235	189	6.0	1.0
12	570	24	234	192	5.4	0.40
		24	214	182	6.1	1.0
	660	75	220	188	7	1.4
		100	220	182	8	1.6
	750	24	185	158	7	1.0
	480	75	177	155	4	1.4
		100	210	177	4.4	1.5
26	570	24	210	185	4.5	0.6
		24	206	179	5.0	2.0
	660	75	173	158	4.3	1.6
		100	176	151	4.7	2.0
	750	24	150	134	5.0	1.20
	840	24	154	126	6.1	0.50
24	480	75	231	190	5.0	1.0
		100	--	189	-	0.7
	660	75	226	194	5.0	1.0
		100	220	182	8	1.4

*Substandard Charpy impact specimens using a 16-ft-lb hammer.

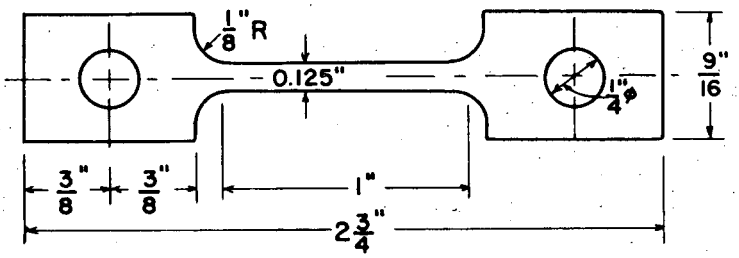

TENSILE SPECIMEN, THICKNESS = 0.06"

(a)

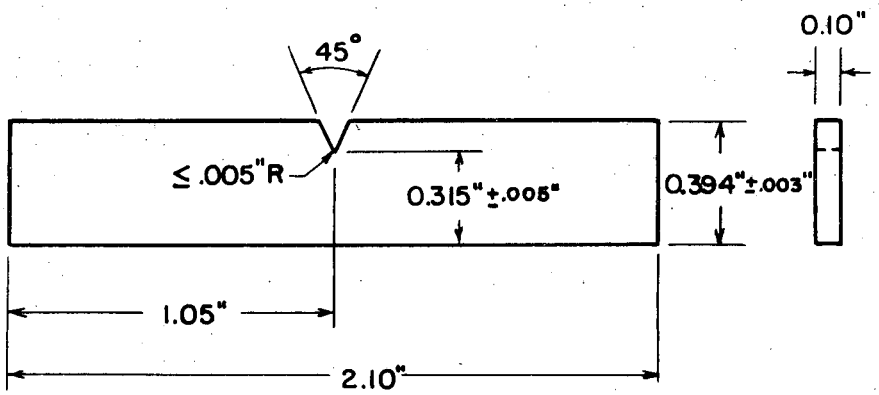

SUBSTANDARD CHARPY IMPACT SPECIMEN.

XBL 6911-6622

(b)

Fig. 1. Dimensions of (a) tensile specimen (b) substandard Charpy impact specimen.

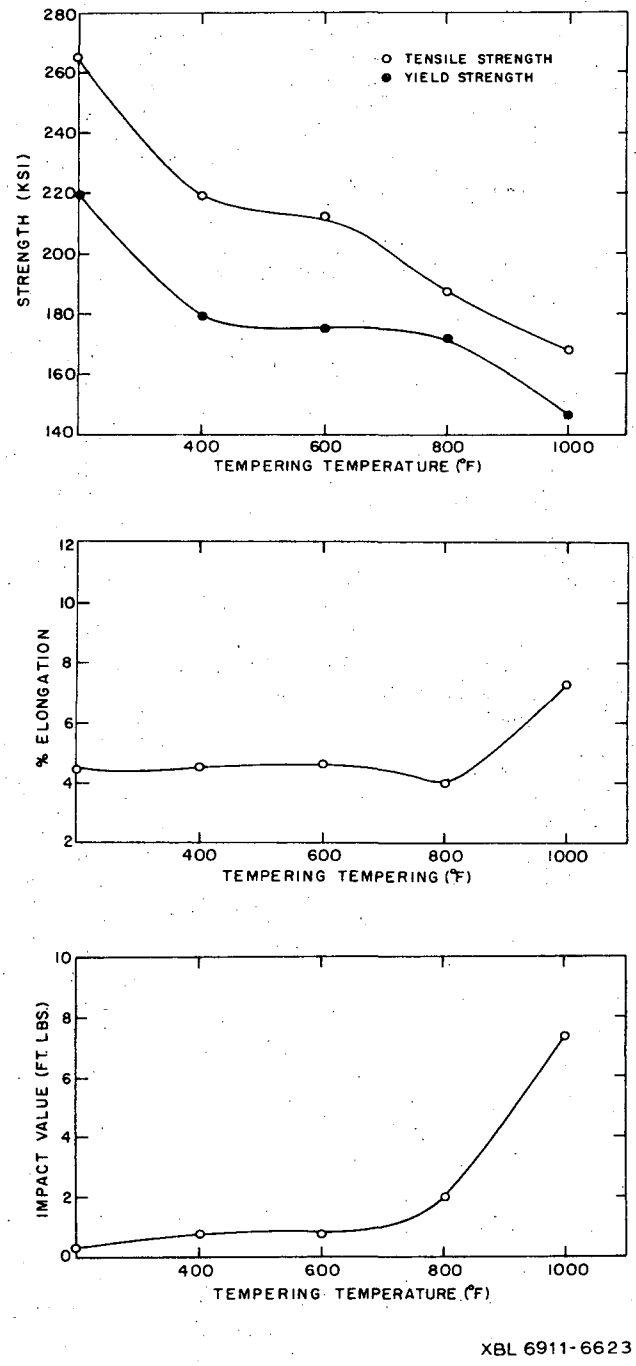

Fig. 2. Effect of tempering on the mechanical properties of Steel 12.

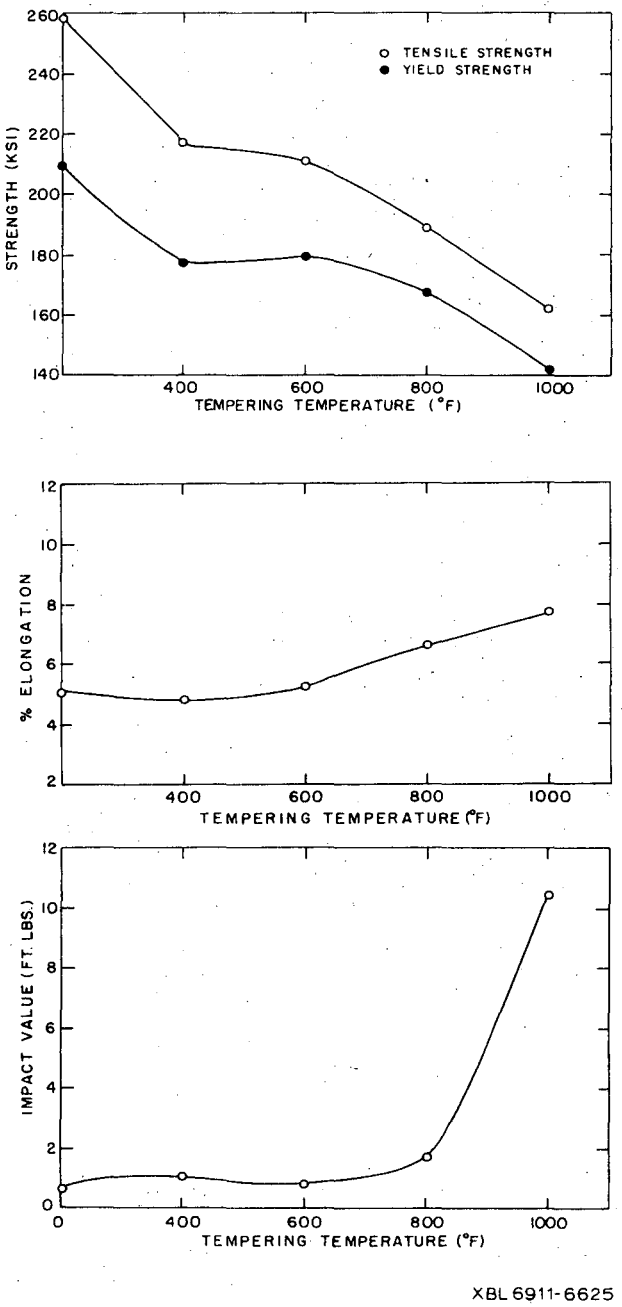

Fig. 3. Effect of tempering on the mechanical properties of Steel 26.

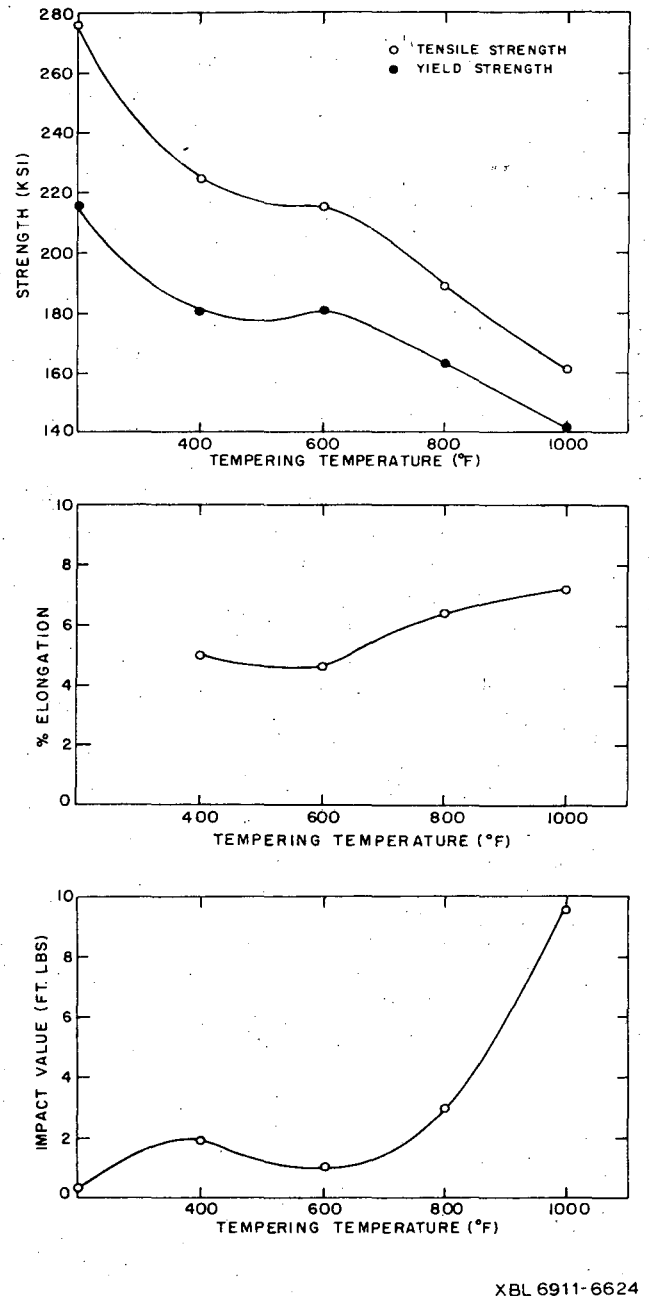

Fig. 4. Effect of tempering on the mechanical properties of Steel 26.

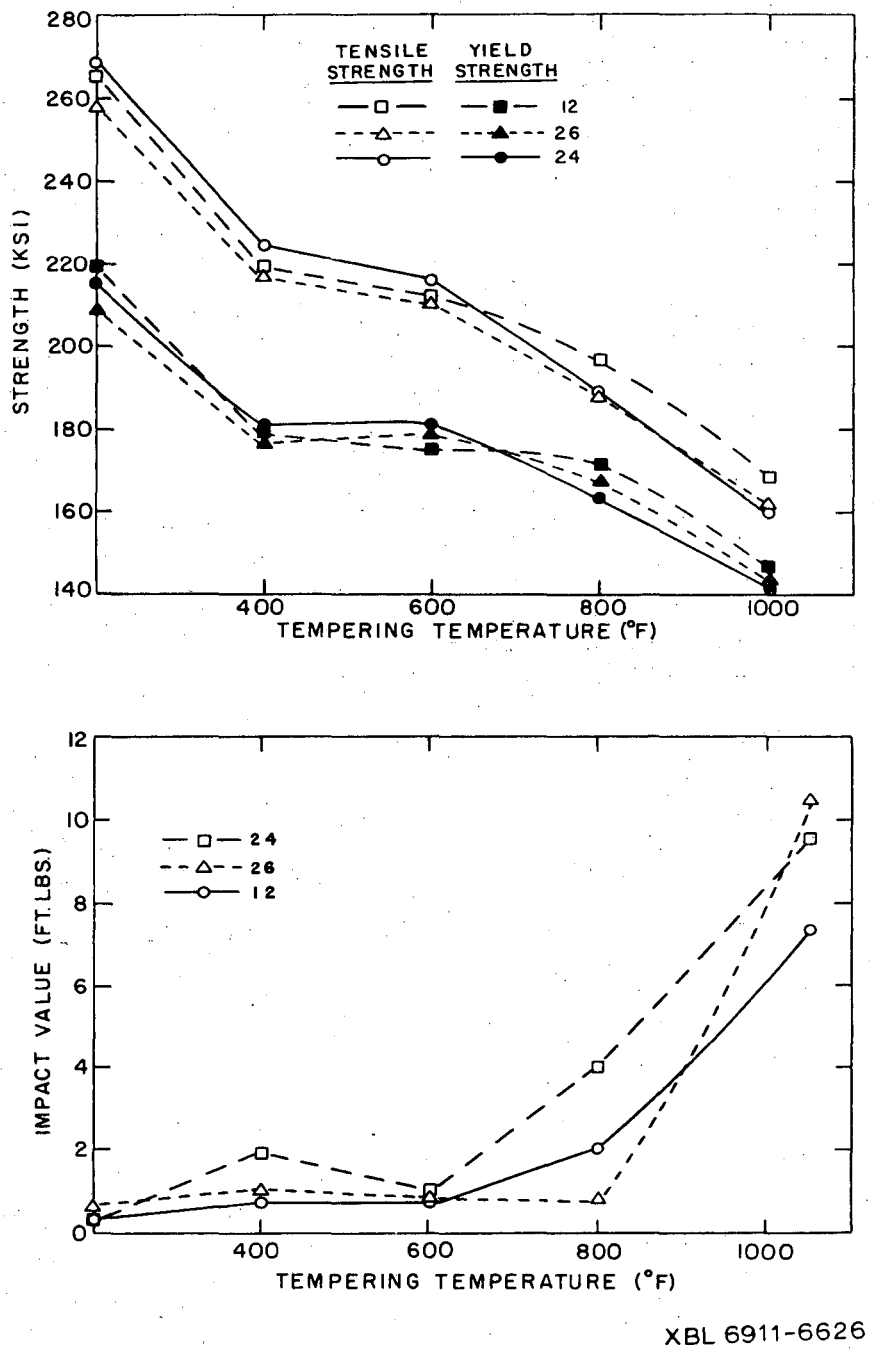

Fig. 5. Effect of tempering on the field strength and notch toughness of the steels.

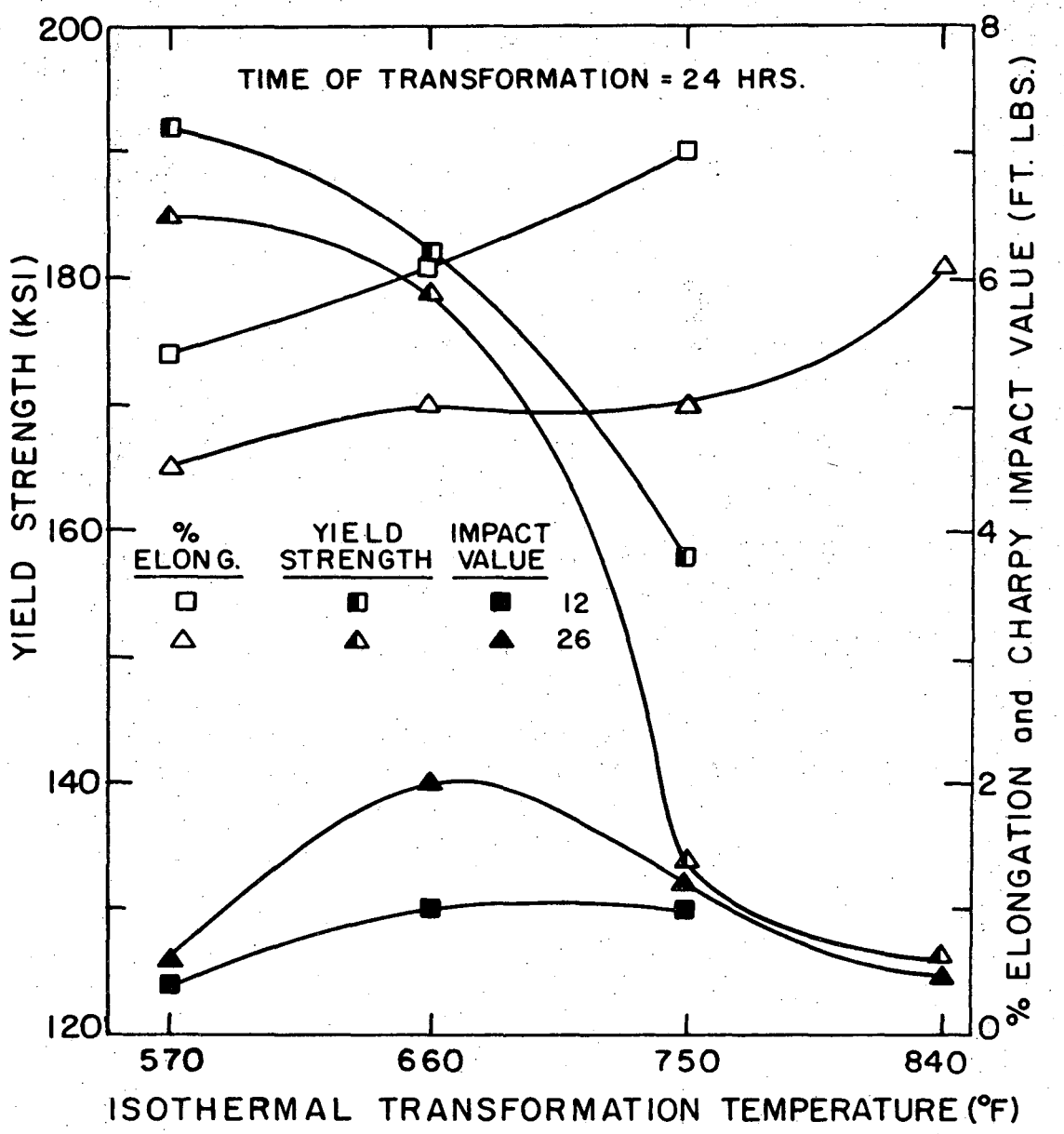

Fig. 6. Effect of isothermal transformation temperature on the mechanical properties of Steel 12 and 26.

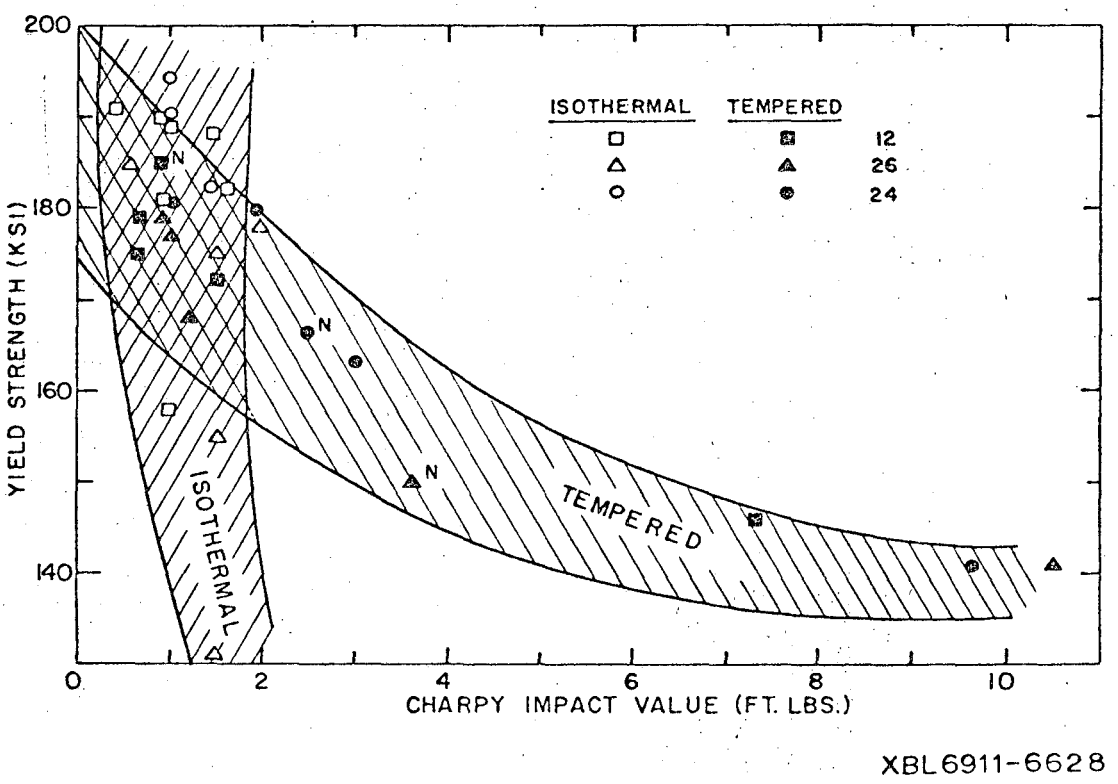

Fig. 7. Yield strength vs notch toughness plot of the heat treated steels.

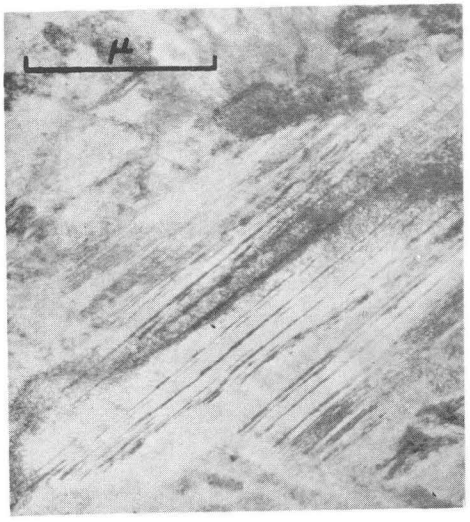

a

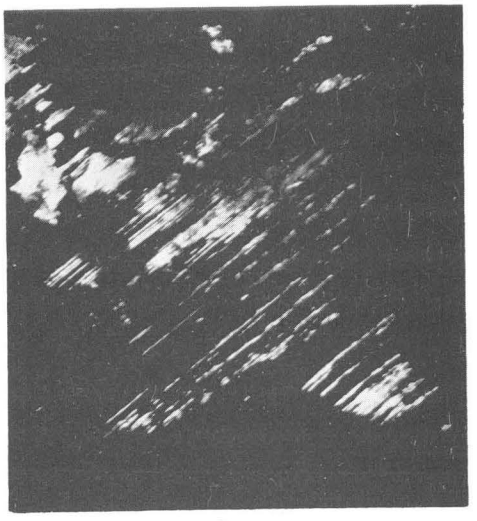

b

c

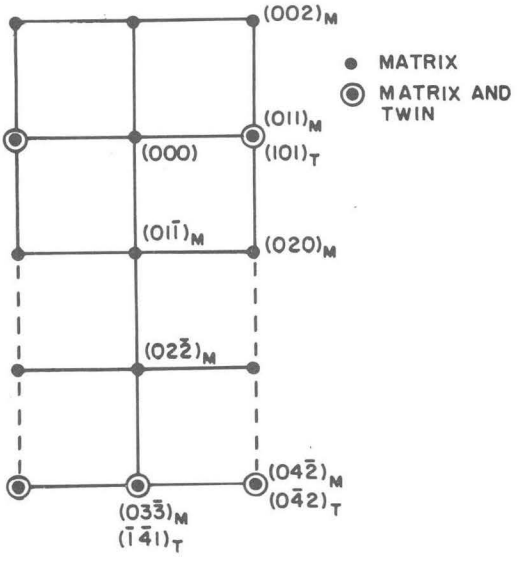

MATRIX ORIENTATION	[100]
TWIN ORIENTATION	[$\bar{2}$12]
TWIN PLANE	(112)

d

XBB 6911-7672

Fig. 8. Martensite of Steel 12. (a) Bright field image showing extensive twins. (b) Dark field image of($\bar{1}$0$\bar{1}$) spot [circled in the pattern (c)] reversing contrast at the twin. (c) Selected area diffraction of the twins in (a). (d) Indexing of diffraction pattern (e).

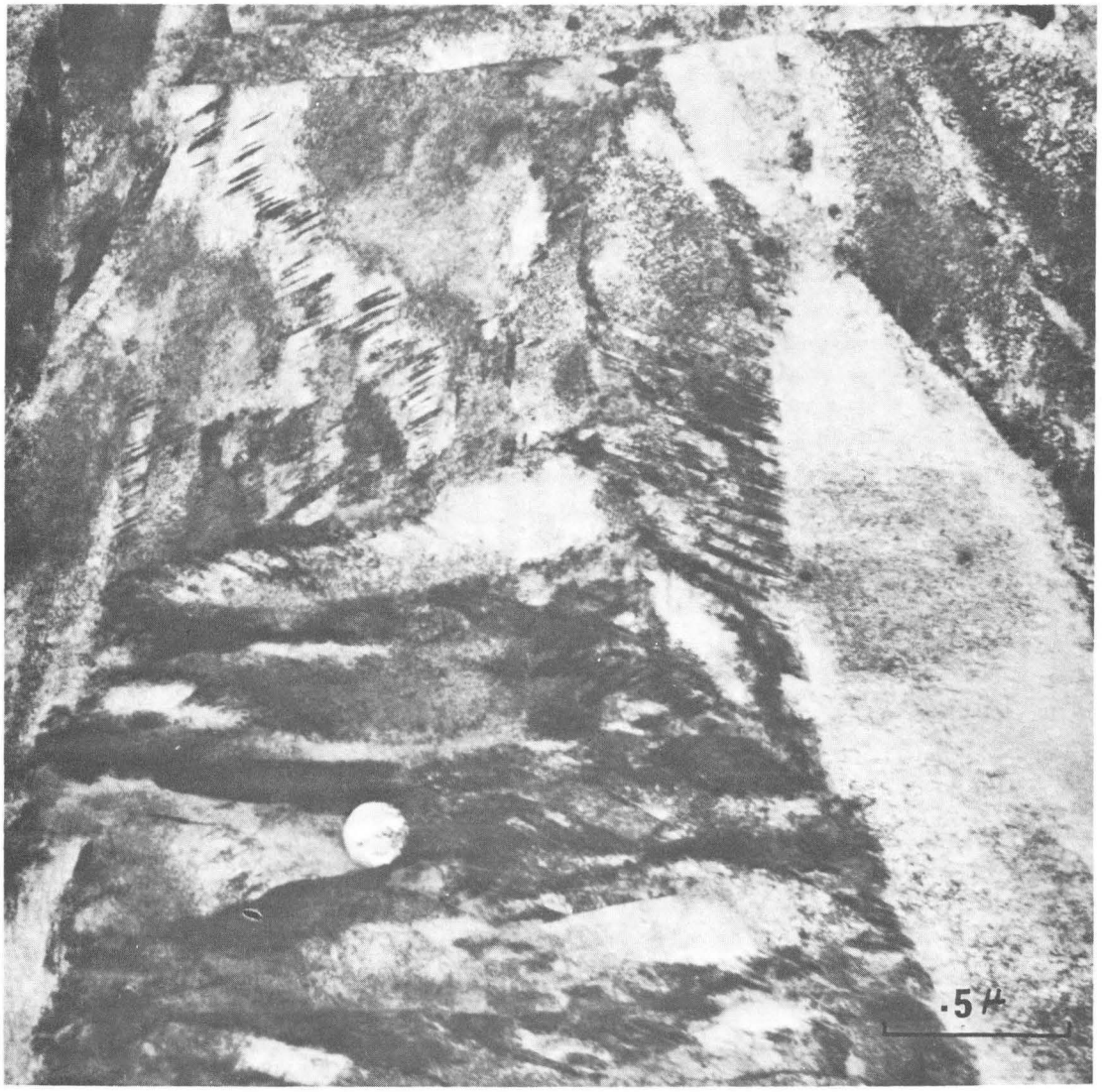

XBB 6911-7671

Fig. 8 (continued) (e) Another region showing fine twins.

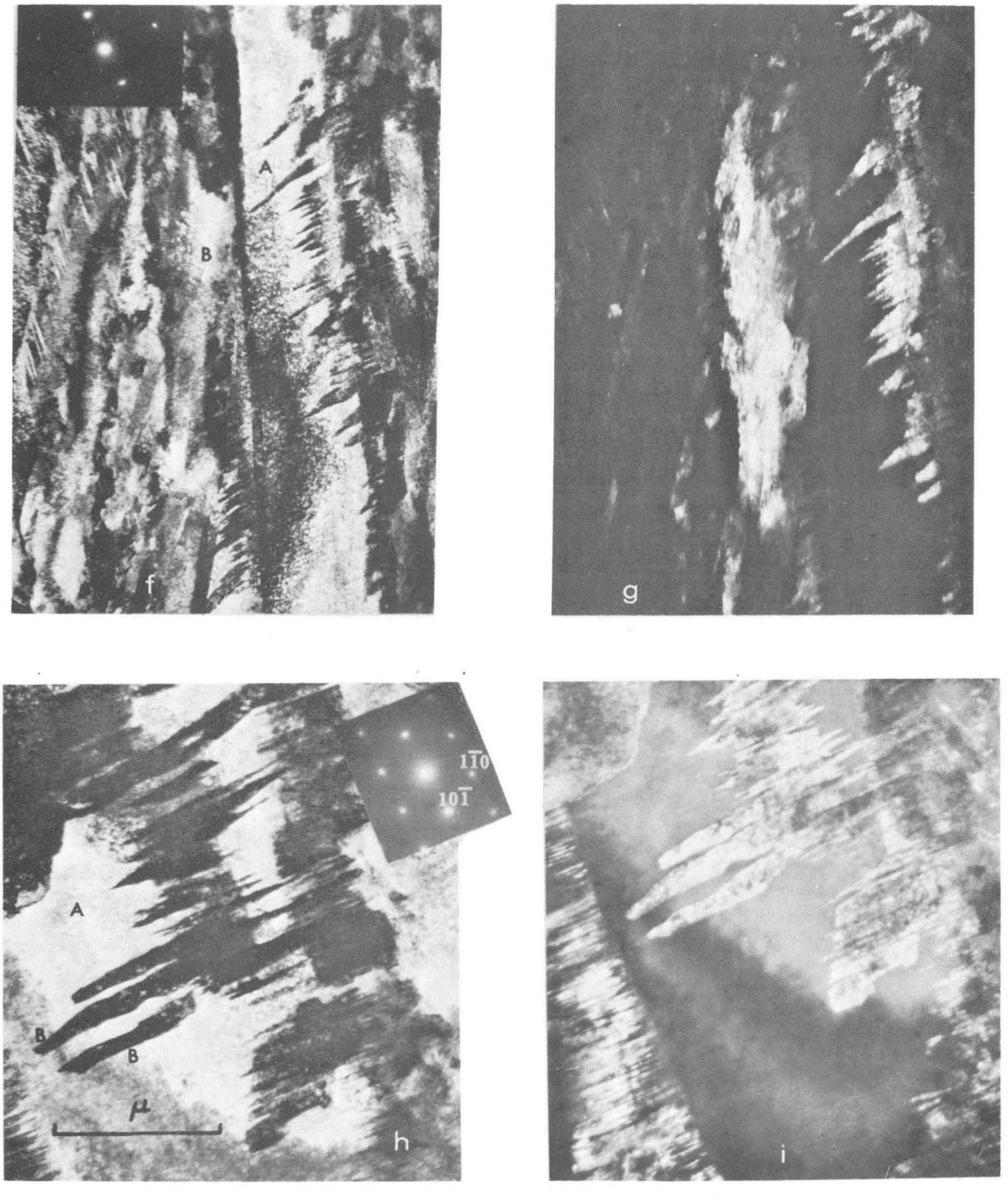

XBB 6911-7665

Fig. 8 (continued) (f) Bright field micrograph showing plates marked A and B, which are twin related. The inset shows the selected area diffraction of the twins in plate A having an [011] orientation. (g) Dark field image of (200) spot [circled in the selected area diffraction of (f)] reversing contrast of the plate B and the twin in plate A. This shows that plates A and B are twin related. (h) Bright field micrograph showing plate A containing twins and some substructures marked B. The inset shows the selected area diffraction of the twins in [111] orientation. (j) The dark field of (1$\bar{1}$0) spot reverses the contrast of the twins and substructures shown in (h). This proves that the substructures are twin related with the plate.

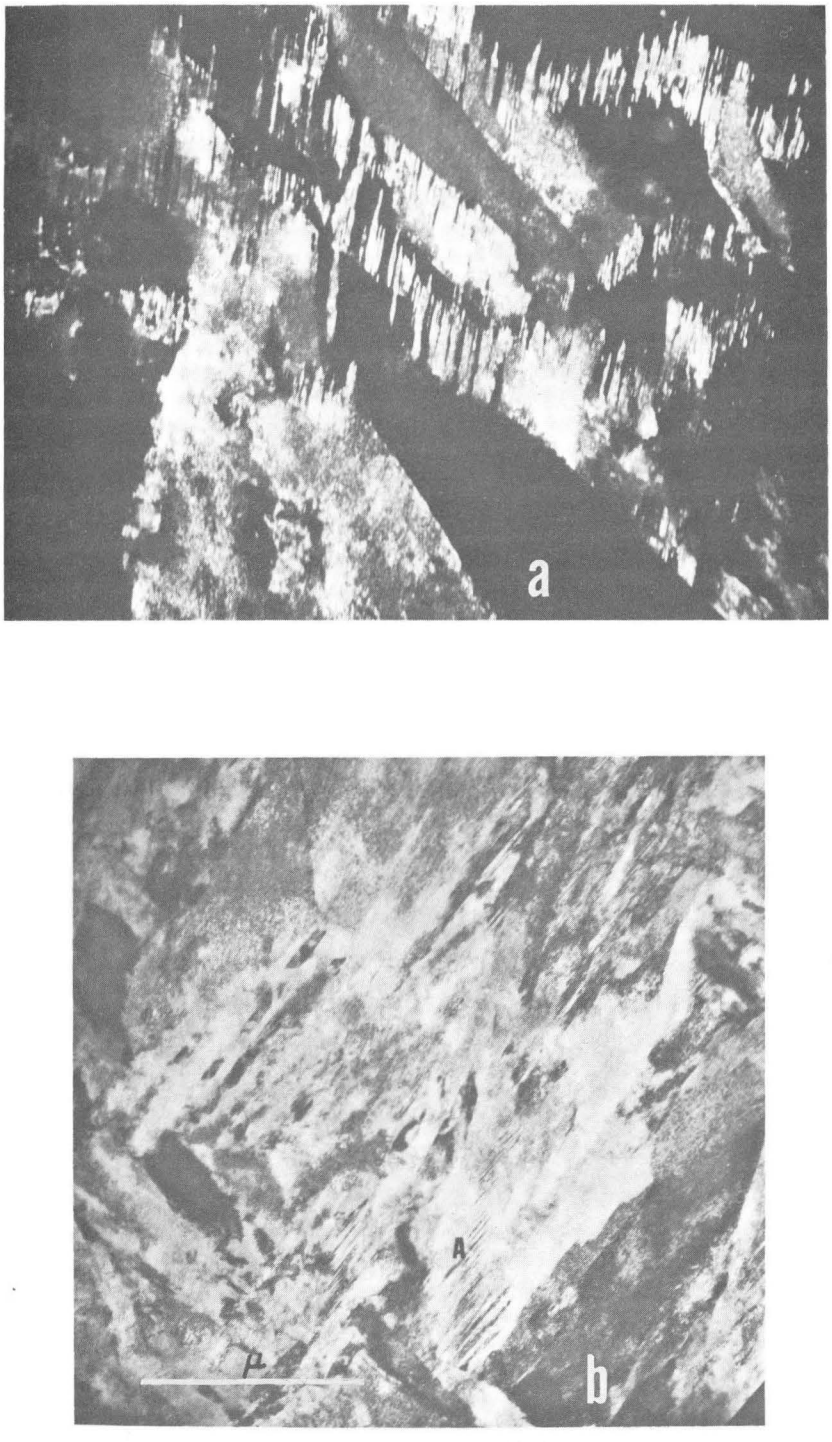

XBB 6911-7667

Fig. 9. Martensite of Steel 26. (a) Dark field micrograph showing reversal of contrast of the twins. (b) Regions showing fine twins marked A.

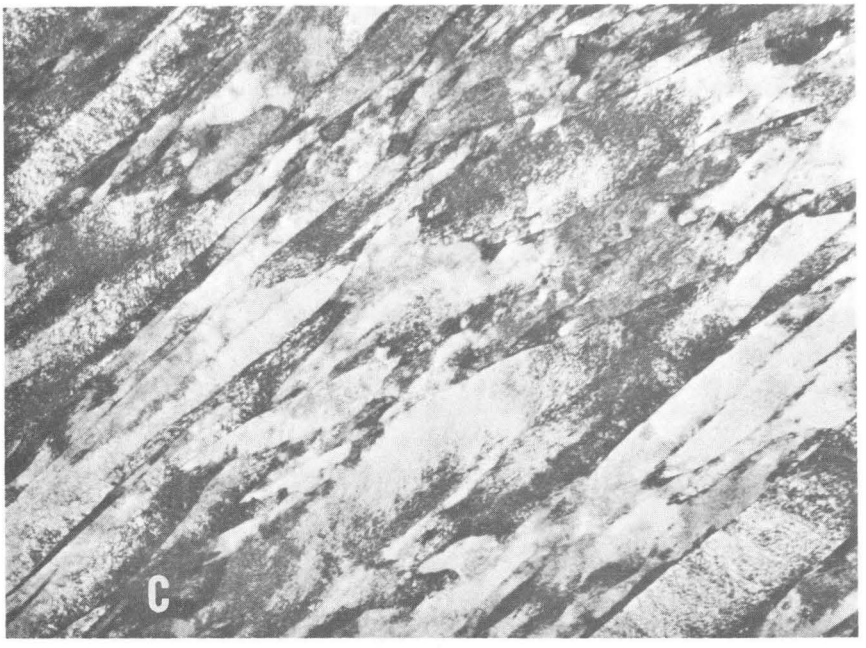

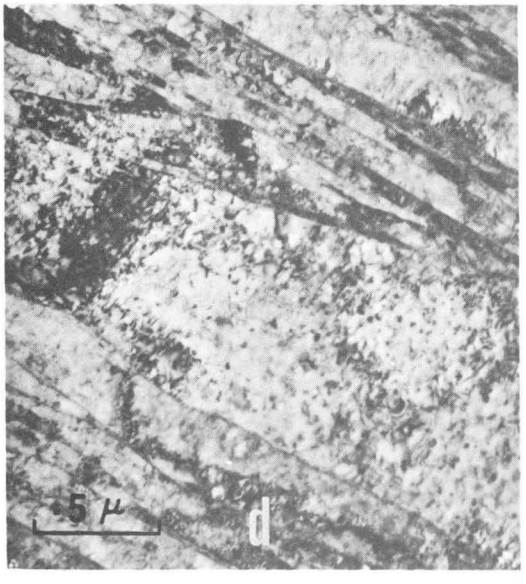

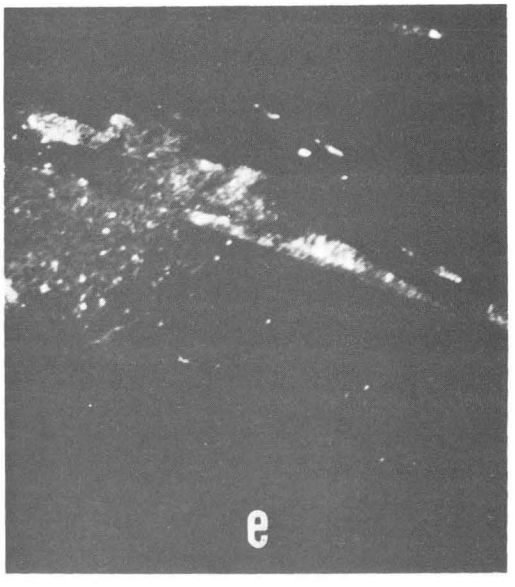

XBB 6911-7669

Fig. 9 (continued) (c) Bright field image showing dislocated martensite. This structure was not frequently observed in this steel. (d) Bright field micrograph of a plate exhibiting autotempered carbide precipitation. (e) Dark field image of a carbide spot reverses the contrast of the spherodized autotempered carbides.

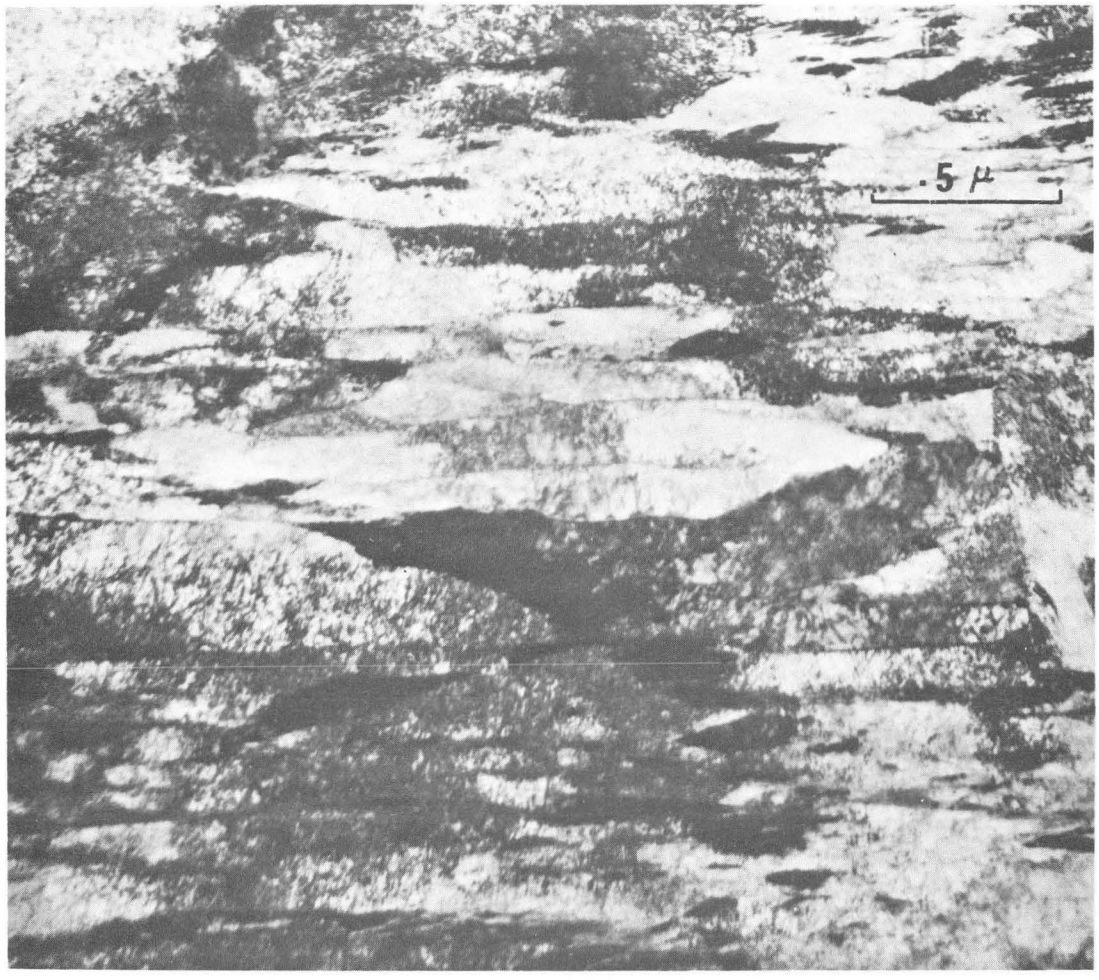

XBB 6911-7659

Fig. 10. Bright field micrograph showing dislocated martensite in Steel 22.

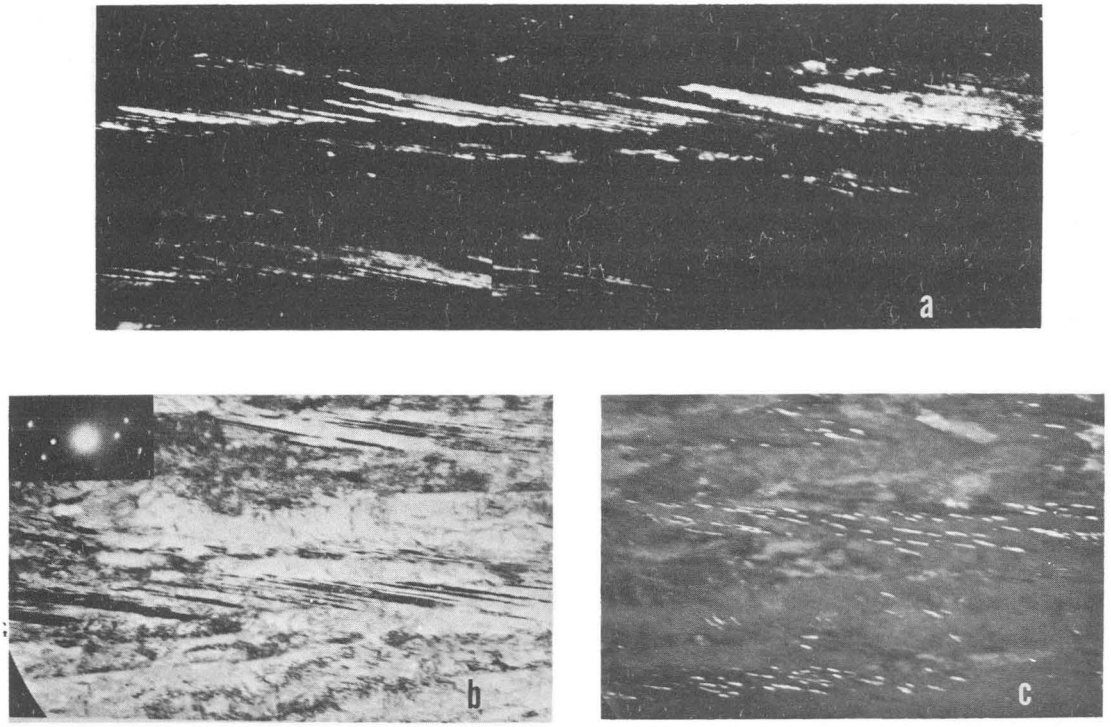

XBB 6911-7658

Fig. 11. Steel 26, quenched and tempered at 400°F for 4 hrs. (a) Dark field image of (110) twin spot [circled in the inset of (b)] reversing contrast of the twins. (b) Bright field micrograph of extensive twins with the inset showing the selected area diffraction pattern. The cementite precipitated along the twins are not clearly visible in the bright field image but in (c) the dark field micrograph of a cementite reflection reversing the contrast of carbides at the twins.

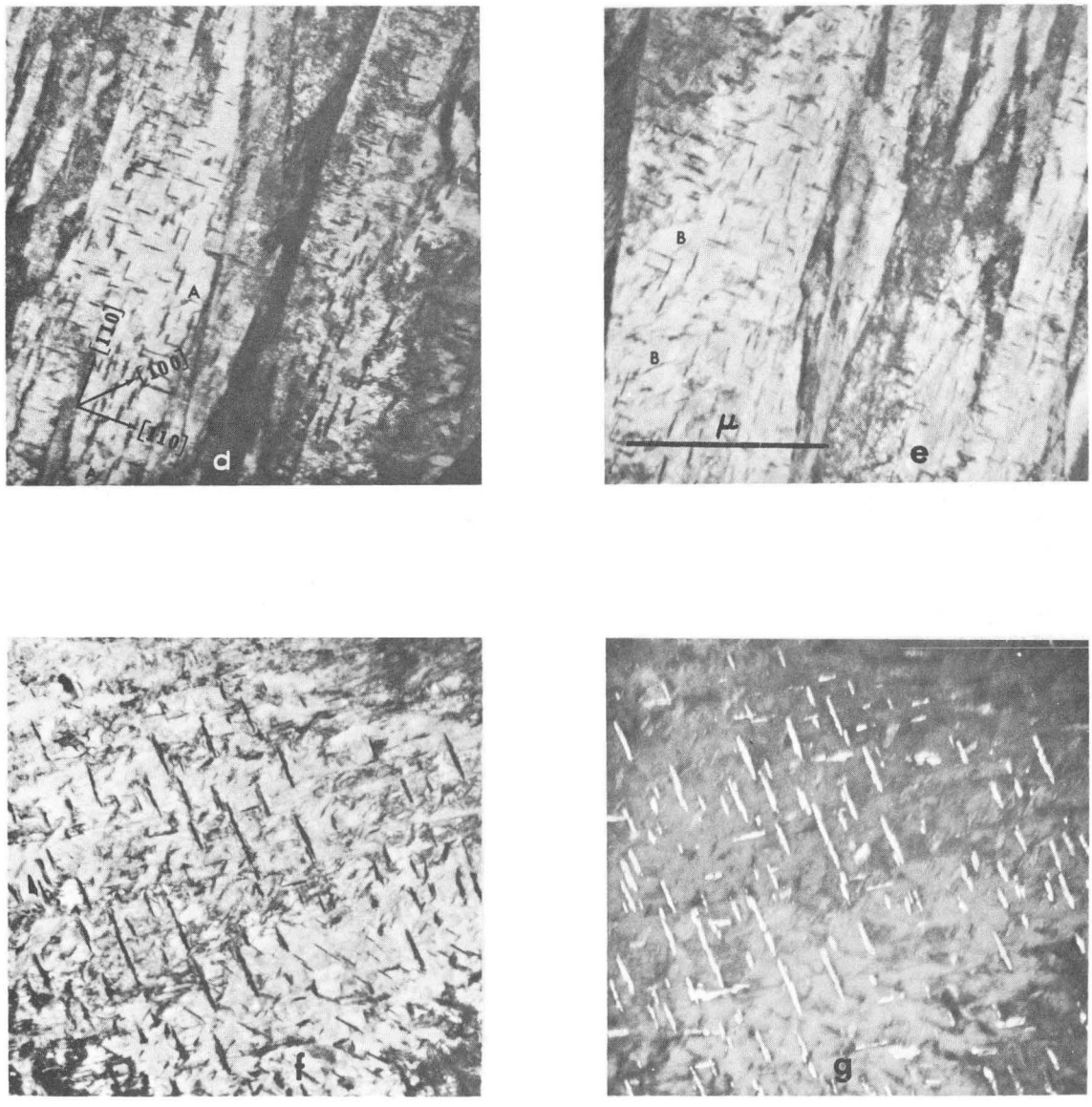

XBB 6911-7662

Fig. 11 (continued) (d) Bright field image of a plate showing two directional sharp precipitates of cementite and wavy ϵ-carbides marked "A". The carbides are identified by trace analysis. (e) Showing cementite precipitation. Regions marked "B" refer to wavy ϵ-carbide precipitates. (f) Shows sharp cementite precipitates in a plate and (g) the dark field micrograph showing reversal of contrast of cementite.

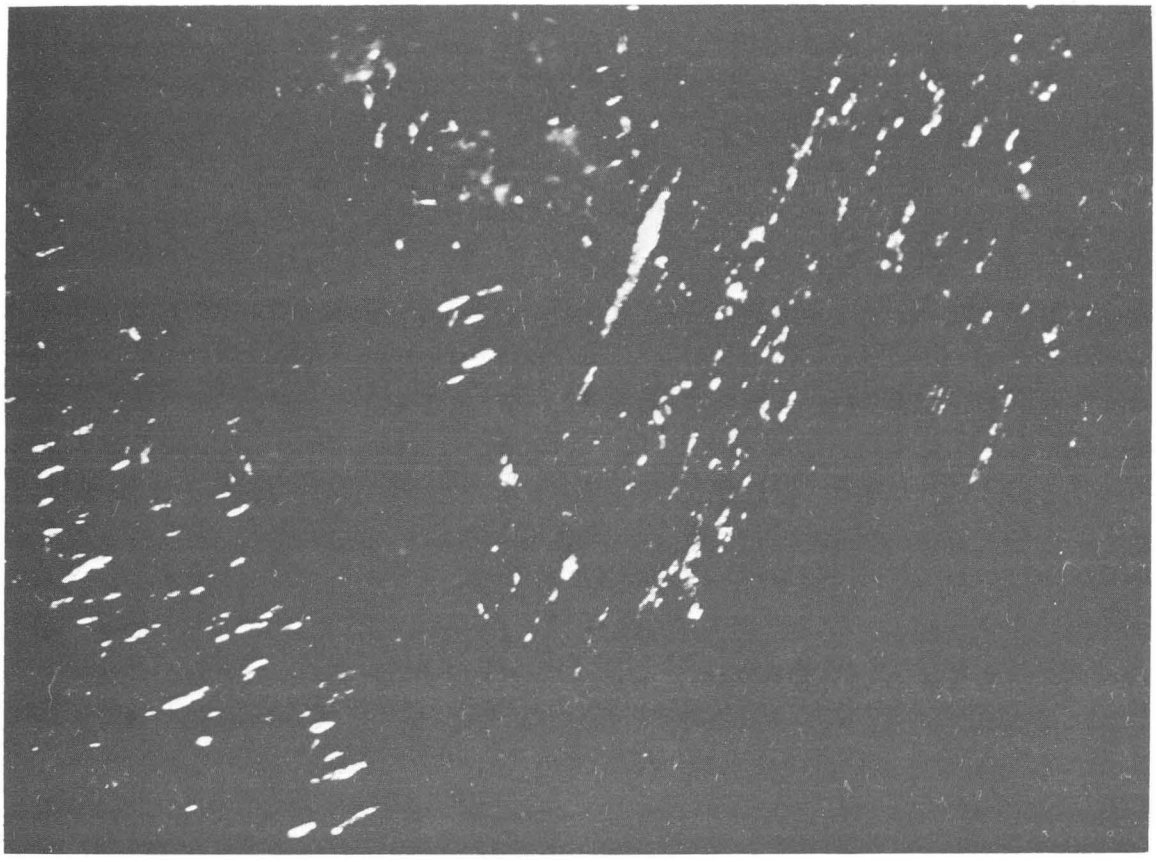

XBB 6912-7683

Fig. 12. Dark field micrograph of a carbide reflection reversing contrast of the carbides formed along the plate boundaries and in the matrix (40,000×) in Steel 26, quenched and tempered at 600°F for 4 hrs.

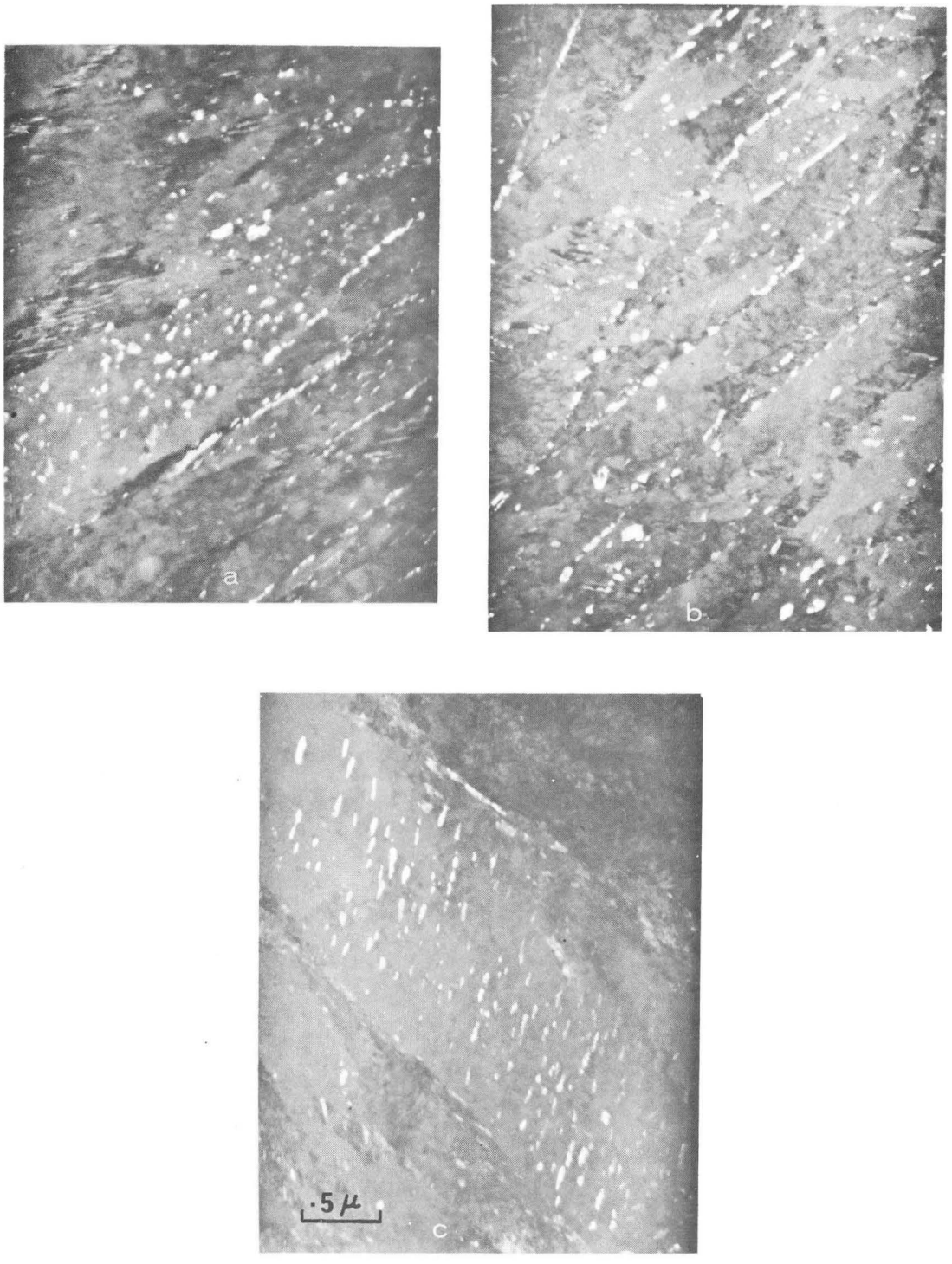

XBB 6911-7664

Fig. 13. Steel 26, quenched and tempered at 800°F for 4 hrs. (a) and (b) Dark field image showing reversal of contrast of coarse carbide precipitation in the matrix (spherodized), on twins and plate boundaries. (c) Dark field micrograph showing reversal of carbides inside a plate.

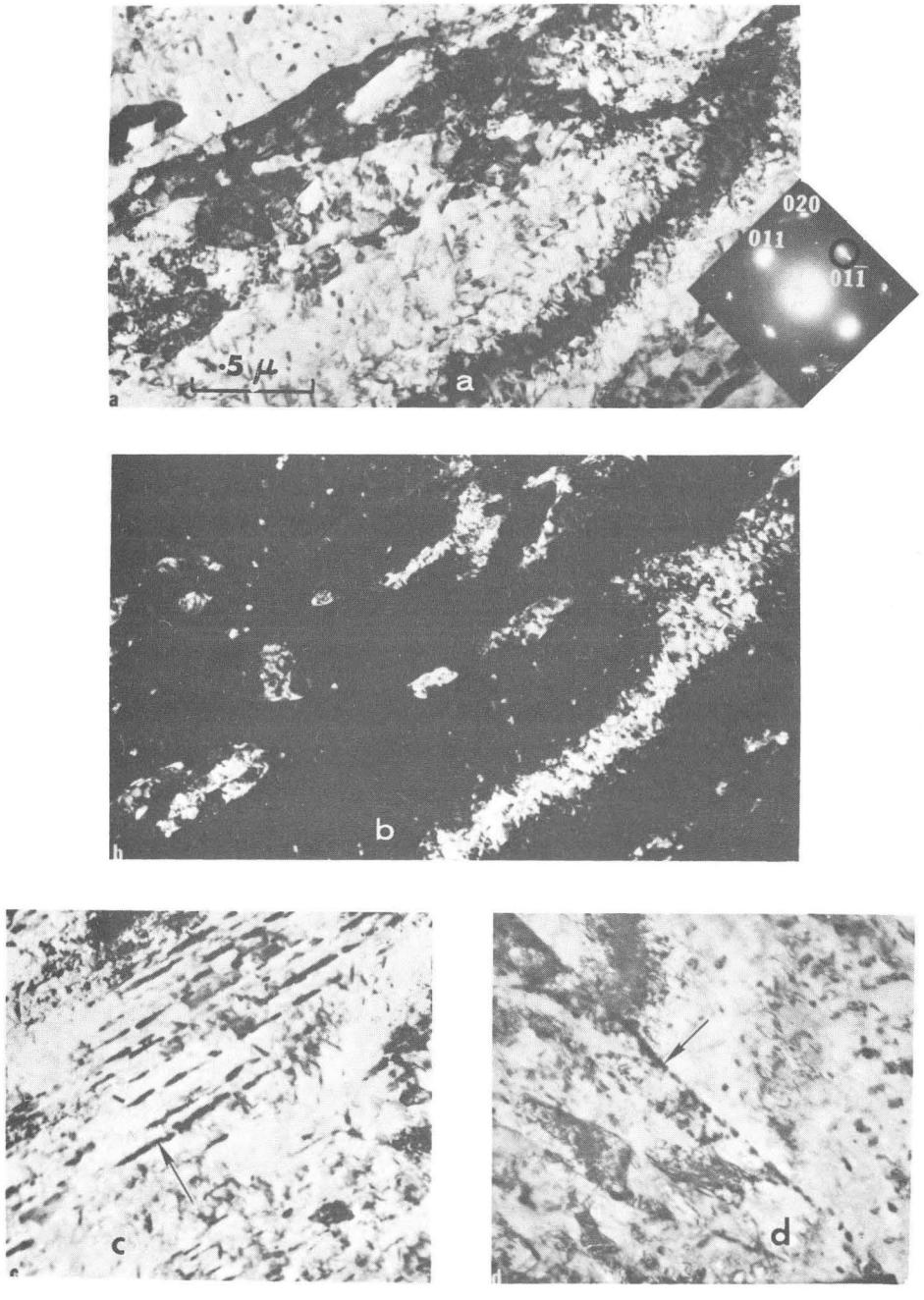

XBB 6911-7668

Fig. 14. Steel 12, quenched and tempered at 1000°F. (a) Bright field micrograph showing spherodized carbides. The inset shows the selected area diffraction pattern having an [100] orientation. (b) Dark field image of (01$\bar{1}$) spot reversing contrast of the matrix and the carbides because a carbide spot is superimposed on the (01$\bar{1}$) matrix spot. (c) Bright field picture showing coarse carbide precipitation along twins (indicated by an arrow) and (d) along grain boundary (indicated by an arrow).

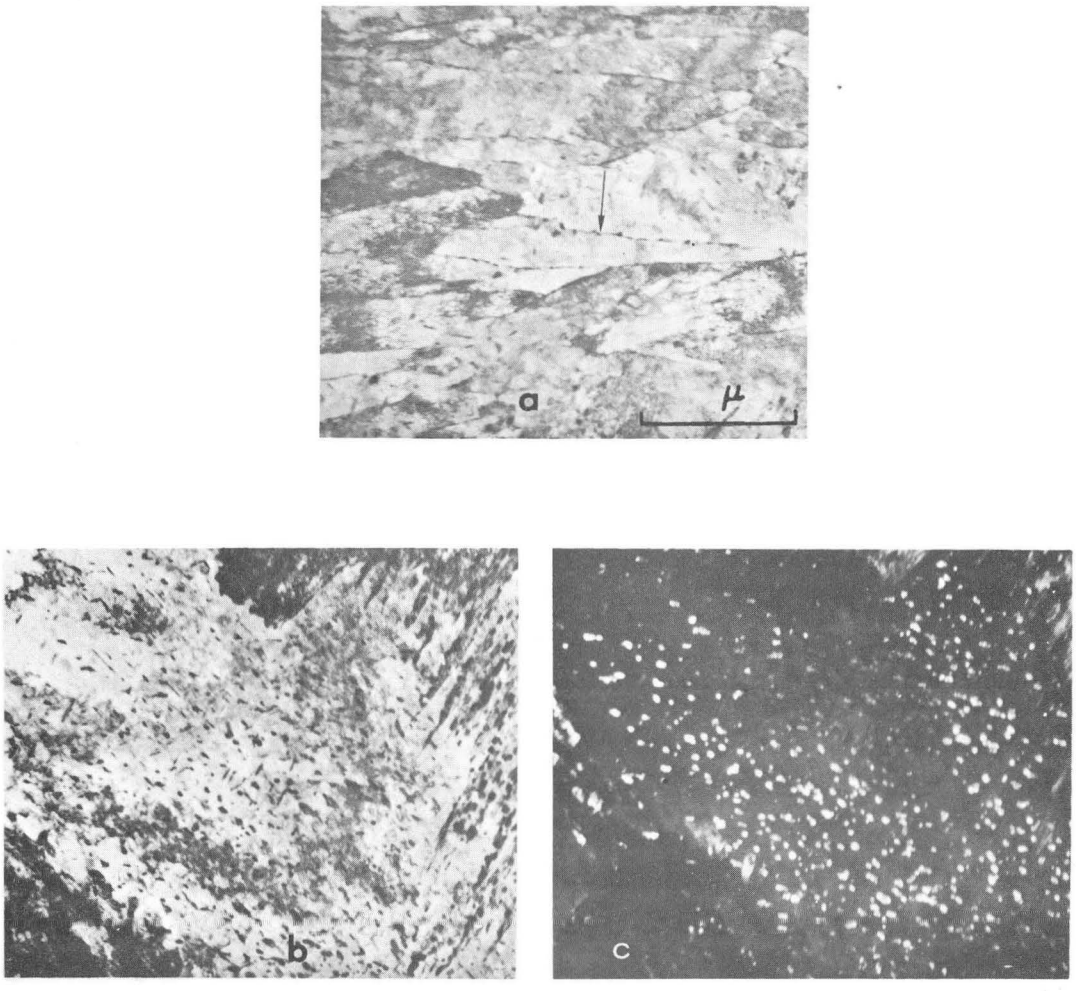

XBB 6911-7675

Fig. 15. Steel 26, quenched and tempered at 1000°F. (a) Bright field image showing carbide precipitation at the plate boundaries (indicated by an arrow). (b) Bright field image showing precipitation of carbides in a plate and along twins (marked A). The carbides reverse contrast in the dark field image (c).

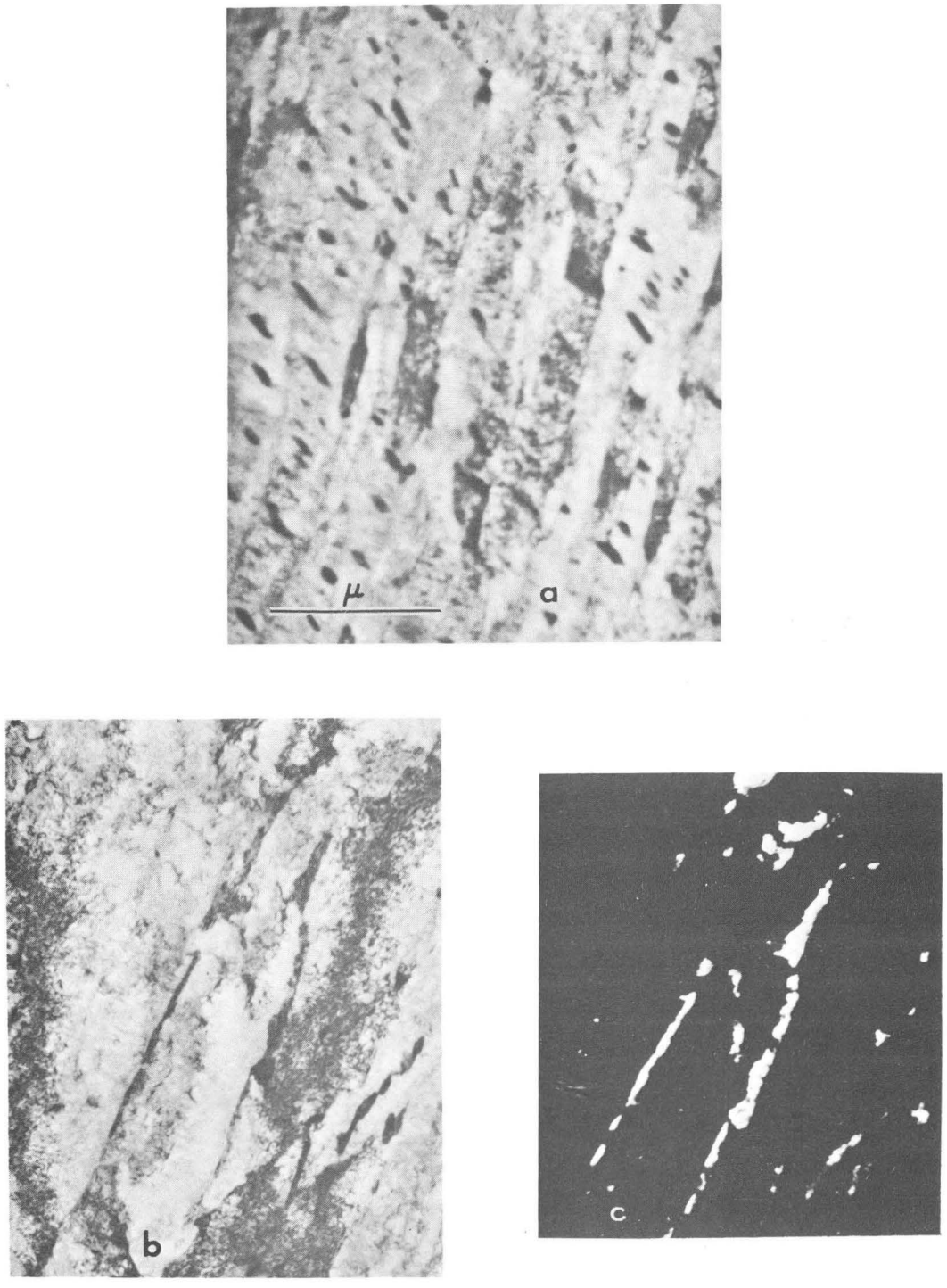

XBB 6911-7661

Fig. 16. Steel 26, isothermally transformed at 750°F for 24 hrs. (a) Bright field image showing lower bainite with cementite at an angle of 55-65° to the long direction of the laths. (b) Regions of upper bainite where cementite forms at the lath boundaries. The cementite reverses contrast in the dark field image (c).

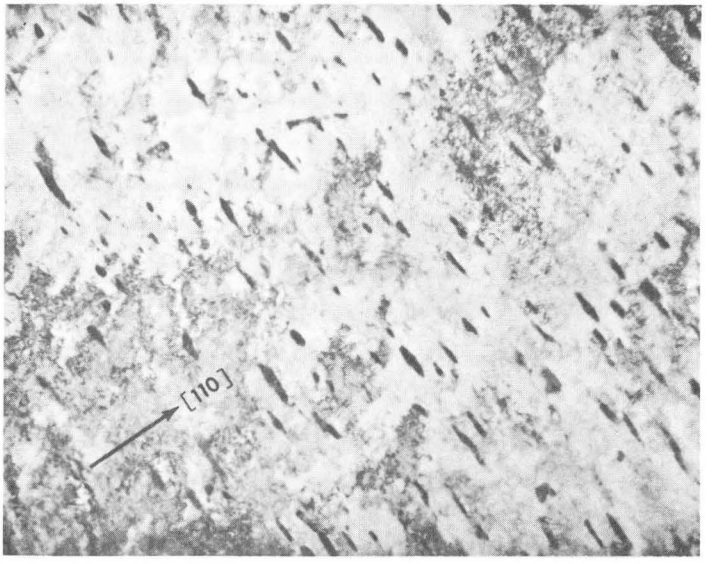

d

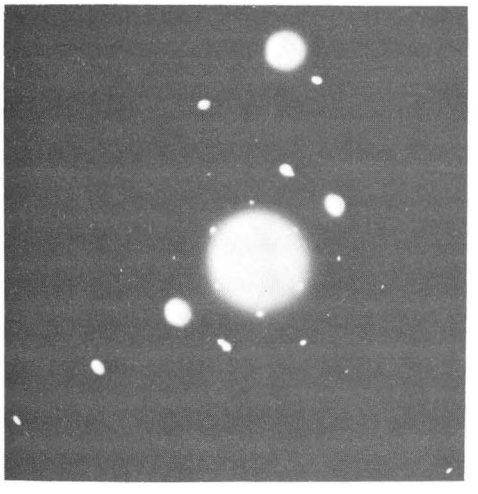

e

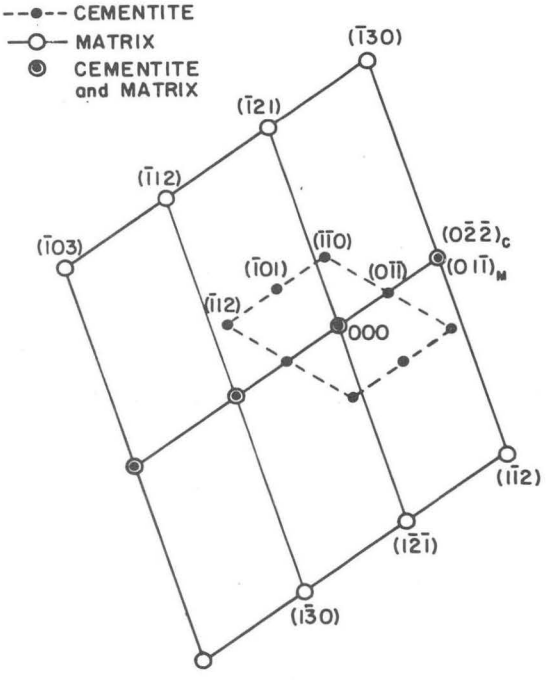

f

XBB 6912-7684

Fig. 16 (continued) (d) Bright field micrograph of lower bainite. (e) Selected area diffraction of lower bainitic carbides. (f) Indexing of diffraction pattern (e).

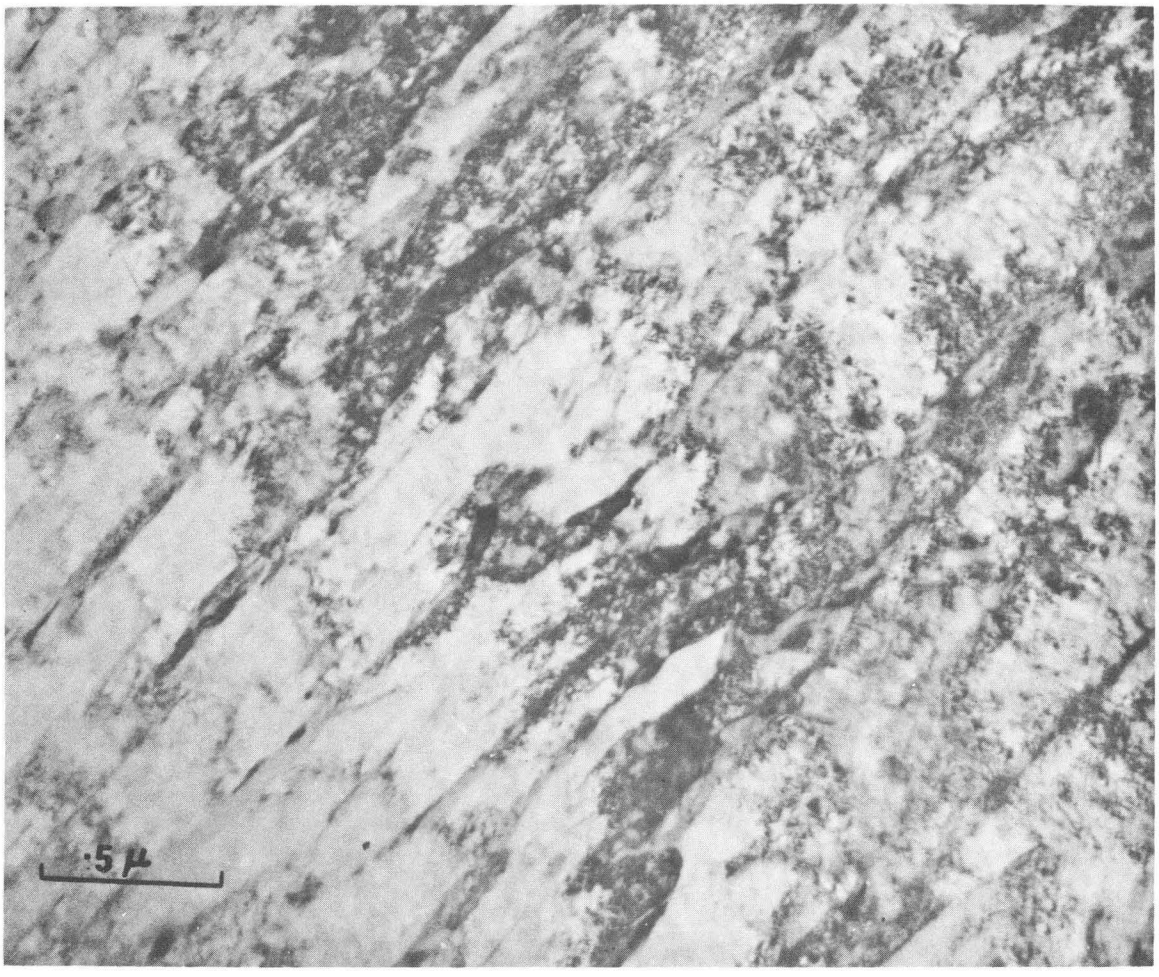

XBB 6911-7674

Fig. 17. Steel 26, isothermally transformed at 840°F for 24 hrs. Bright field image shows upper bainitic laths with carbides along the lath boundaries (carbides not in contrast).

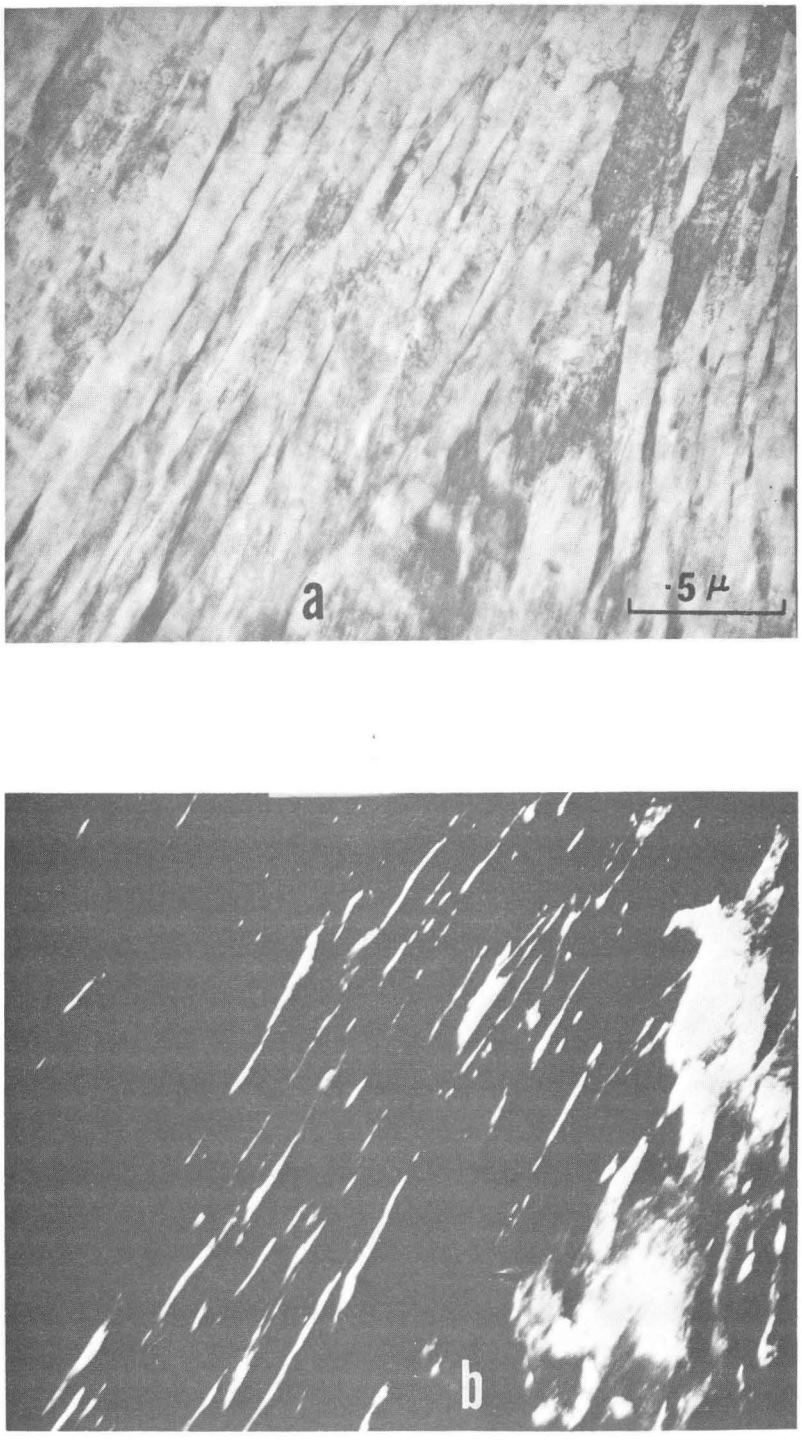

XBB 6911-7670

Fig. 18. Steel 12, continuously cooled. (a) Bright field image of upper bainite. The carbides reverse contrast in the (b) dark field image.

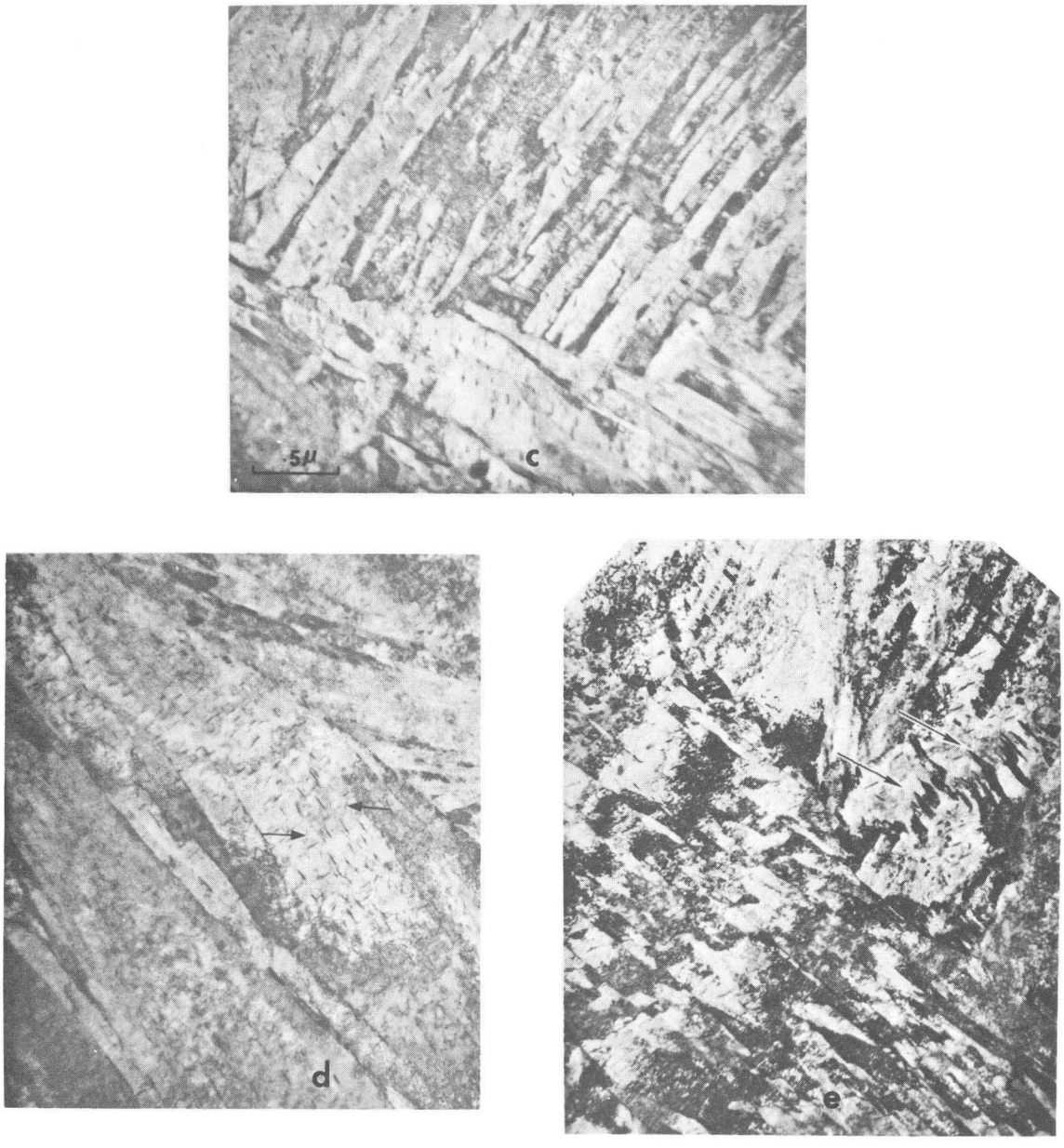

XBB 6911-7660

Fig. 18 (continued) (c) Bright field image of lower bainite showing two directional laths. (d) Bright field micrograph of a tempered martensitic plate showing sharp cementite precipitates and wavy ϵ-carbide (marked by arrows) (e) Bright field image showing regions of twinned martensite (marked by arrows).

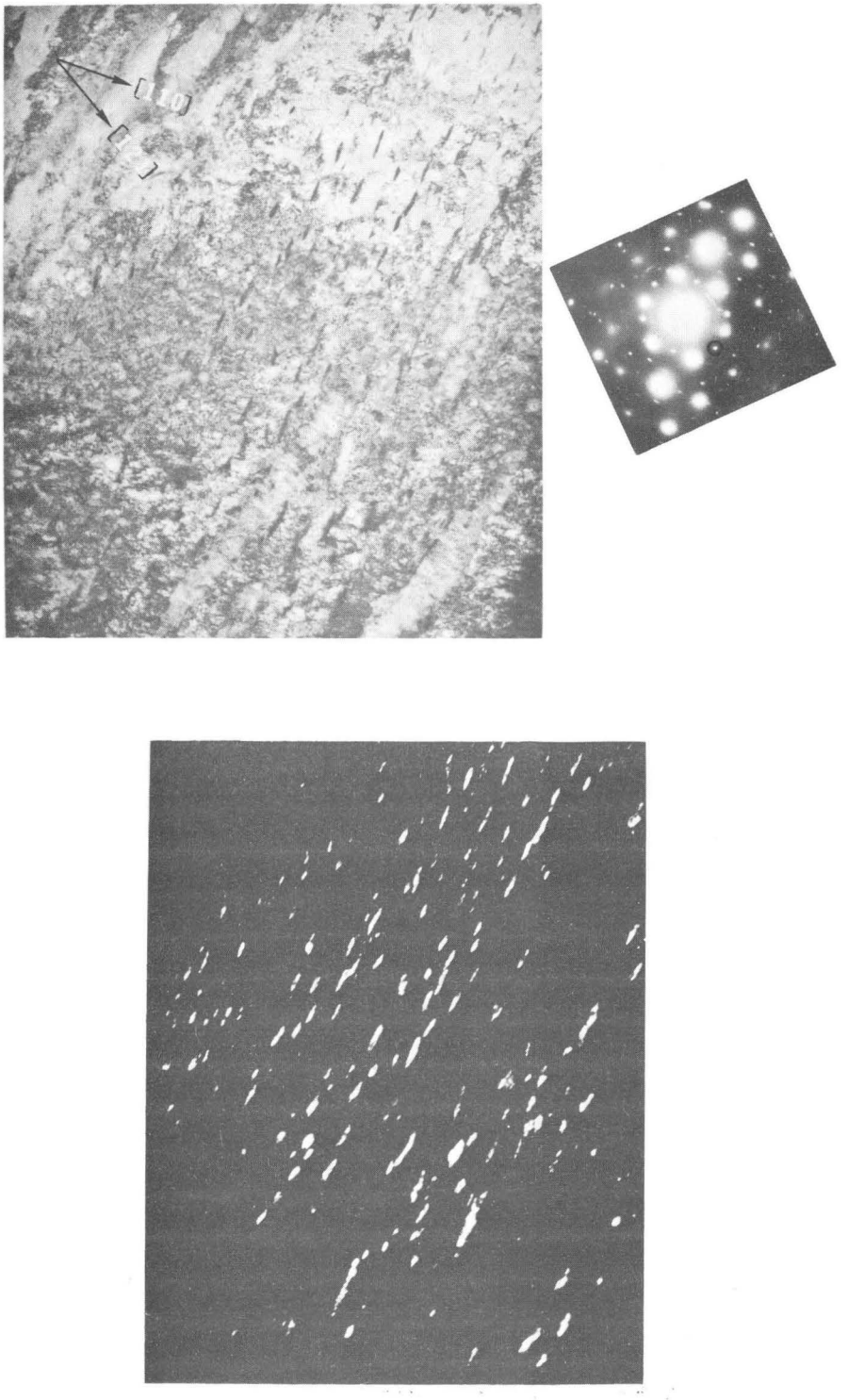

XBB 6911-7663

Fig. 19. Steel 26, continuously cooled. (a) Bright field image of lower bainite and (b) the dark field image where cementite reverses contrast.

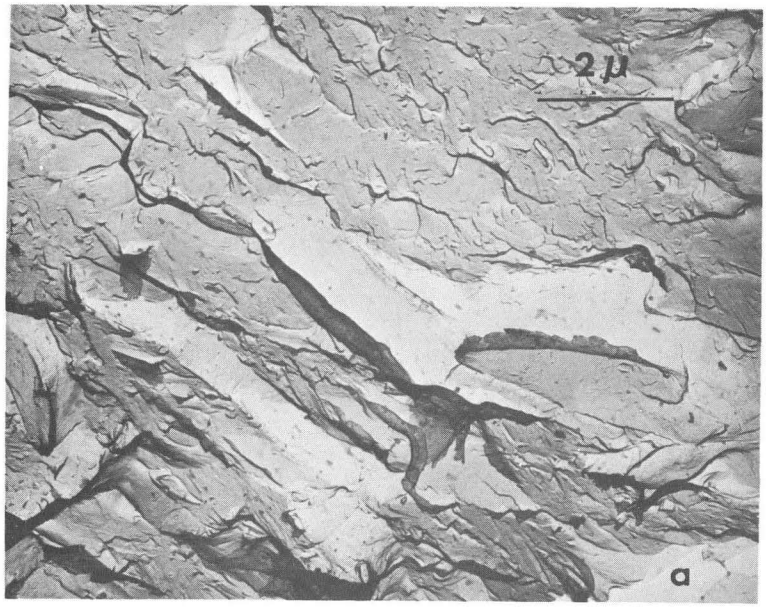

XBB 6911-7666

Fig. 20. (a) Replica fractograph of martensite of Steel 12 showing cleavage failure. (b) Replica fractograph of Steel 12 quenched and tempered at 1000°F showing dimple rupture.

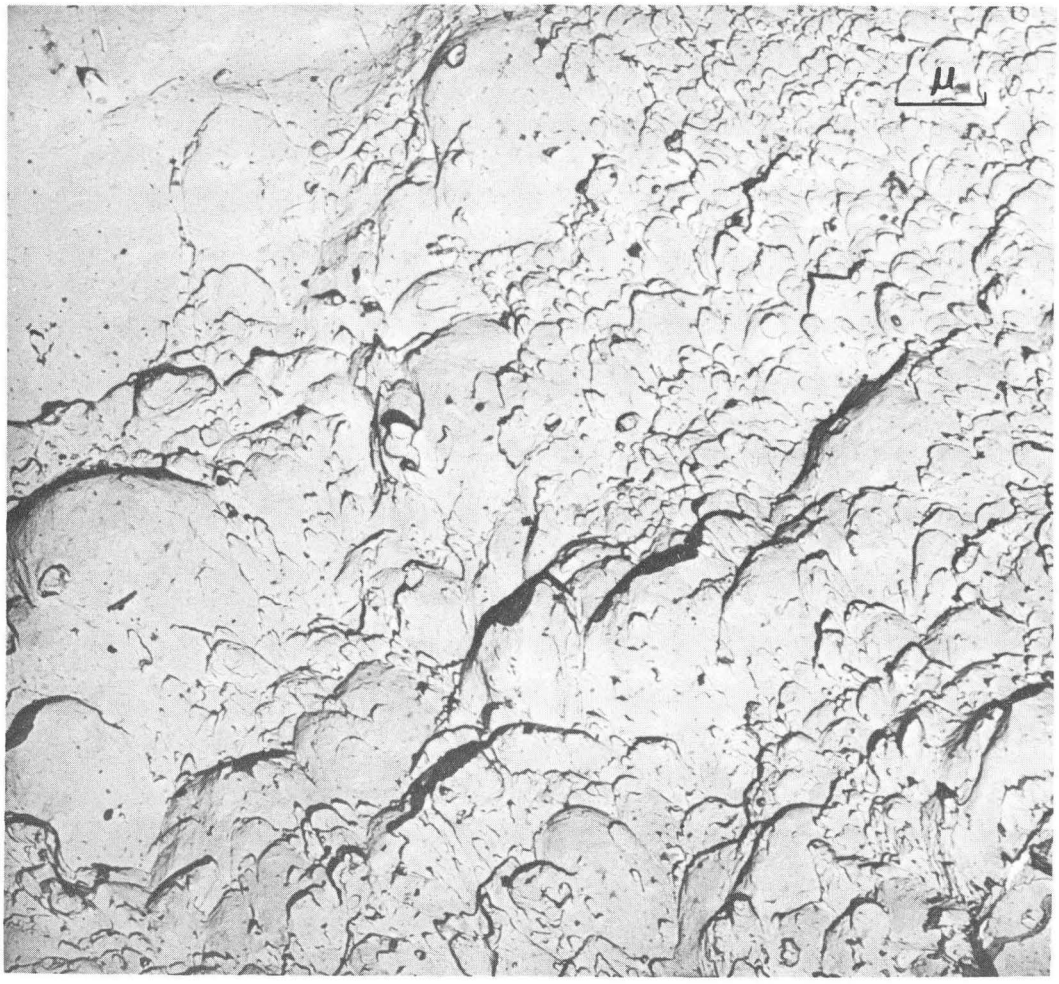

XBB 6911-7673

Fig. 21. Replica fractograph of Steel 12 quenched and tempered at 600°F showing dimple rupture.

TECHNICAL INFORMATION DIVISION
LAWRENCE RADIATION LABORATORY
UNIVERSITY OF CALIFORNIA
BERKELEY, CALIFORNIA 94720